Biogeosciences Discuss., 8, 9535–9576, 2011
www.biogeosciences-discuss.net/8/9535/2011/
doi:10.5194/bgd-8-9535-2011

Biogeosciences Discussions

Insignificant enhancement of export flux in the highly productive Subtropical Front, east of New Zealand: a high resolution study of particle export fluxes based on ^{234}Th:^{238}U disequilibria

K. Zhou[1], S. D. Nodder[2], M. Dai[1], and J. A. Hall[2]

[1]State Key Lab of Marine Environmental Science, Xiamen University, Xiamen, China
[2]National Institute of Water and Atmospheric Research Ltd. (NIWA), Private Bag 14-901, Wellington, New Zealand

Received: 10 September 2011 – Accepted: 13 September 2011
– Published: 21 September 2011

Correspondence to: M. Dai (mdai@xmu.edu.cn)

Published by Copernicus Publications on behalf of the European Geosciences Union.

Abstract

We evaluated the downward Particulate Organic Carbon (POC) export fluxes in the Subtropical Frontal zone (STF) of the Southern Ocean. The site is characterized by enhanced primary productivity which has been suggested to be stimulated through so-called natural iron fertilization processes at its northern boundary where iron-depleted subantarctic water (SAW) mixes with oligotrophic, iron-replete subtropical water (STW). We adopted the small-volume ^{234}Th method to achieve highest spatial sampling resolution as possible based on a cruise to the STF to the east New Zealand in austral late autumn-early winter, May–June 2008. The inventories of fluorescence, particulate ^{234}Th and POC observed in the upper 100 m were all elevated in the mid-salinity part of the water type ($34.5 < S < 34.8$), compared with low ($S < 34.5$) and high ($S > 34.8$) salinity waters. However, Steady-State ^{234}Th fluxes were similar cross all of the salinity gradient being 1484 in the mid-salinity, and 1761 and 1304 dpm m^{-2} d^{-1} in the high and low salinity zones respectively. Bottle POC/Th ratios at the depth of 100 m were used to convert the Th fluxes into POC export flux. The POC flux was again not enhanced in the mid-salinity range where the primary production was highest, being 7.4 mmol C m^{-2} d^{-1} as compared to 9.9 mmol C m^{-2} d^{-1} in high salinity waters, and 5.9 mmol C m^{-2} d^{-1} in low salinity waters. This study implied that natural iron fertilization does not necessarily lead to the enhancement of POC export in STF regions.

1 Introduction

The Subtropical Front (STF) is a circum-global oceanographic feature, typically between about 35° S and 45° S, where cold, high macro-nutrient, iron-limited subantarctic waters (SAW) mix with warm, low macro-nutrient, subtropical waters (STW) (Longhurst, 1998; Orsi et al., 1995). A number of studies have shown enhanced year-round chlorophyll concentrations and primary production (PP) in this STF region (Behrenfeld and Falkowski, 1997; Comiso et al., 1993; Murphy et al., 2001). The

BGD
8, 9535–9576, 2011

observed PP in the STF, east of New Zealand can be as high as 22 mmol C m^{-2} d^{-1} in winter, which may be more than 4 and 2-fold higher than in the adjacent SAW and STW, respectively (Bradford-Grieve et al., 1997). Similarly elevated integrated production rates have been observed in the STF around 152° E off Australia in summer (Clementson et al., 1998) and in the South African sector at 20° E in winter (Froneman et al., 1999). Such enhancement in PP in the STF zone has been suggested to be induced by natural iron fertilization processes, with the iron sourced from atmospheric deposition, shelf boundary exchange processes and/or mixing with iron-replete subtropical waters (Boyd et al., 1999, 2004; Pollard et al., 2009).

To the east of New Zealand, the STF is constrained bathymetrically along a prominent submarine ridge, the Chatham Rise (Heath, 1985; Uddstrom and Oien, 1999; Sutton, 2001). Like other STF zones, this site is the transition zone from oligotrophic STW in the north, characterized by the relatively high temperatures (summer >18 °C; winter >14 °C), salinities (>35.1) and dissolved iron levels (>0.2 nmol l^{-1}), and low macronutrient concentrations (e.g. PO_4 < 0.3 µmol l^{-1}), to the high nutrient-low chlorophyll (HNLC) SAW to the south, with typically low temperatures (summer <14 °C; winter <10 °C), salinities (<34.6) and iron levels (<0.1 nmol l^{-1}), and high macronutrient concentrations (e.g. PO_4 > 0.9 µmol l^{-1}) (Boyd et al., 1999; Nodder, 1997). Regardless of seasonal and spatial variations, phytoplankton biomass and biological productivity are generally elevated over the Chatham Rise (Bradford-Grieve et al., 1997, 1999; Gall et al., 1999). In winter and spring, average chlorophyll-*a* concentrations, integrated down to 100 m, can reach up to 79 mg m^{-2}, and the corresponding PP, integrated to 1 % light level, could be more than 52 mmol C m^{-2} d^{-1} (Bradford-Grieve et al., 1997). In comparison, the average inventory of chlorophyll-*a* and PP may be only 13 mg m^{-2} and 12 mmol C m^{-2} d^{-1}, respectively, in SAW and 33 mg m^{-2} and 46 mmol C m^{-2} d^{-1} in STW. Such perennially high PP levels in the STF support a diverse planktonic and benthic ecosystem (Probert and McKnight, 1993; Bradford-Grieve et al., 1999) that seems to be translated to many fish species, with New Zealand's richest deep-water fisheries, primarily in blue grenadier (known locally as hoki, *Macruronus novaezelandiae*)

BGD
8, 9535–9576, 2011

and orange roughy (*Hoplostethus atlanticus*), occurring on the Chatham Rise (New Zealand Ministry of Fisheries, 2009).

However, little is known thus far about the spatio-temporal variability and magnitude of the downward export of particulate organic carbon (POC), or the fate of the PP in this frontal zone. Nodder (1997) used free-floating cylindrical sediment trap moorings in the vicinity of STF to show that POC flux was less than 3 mmol C $m^{-2} d^{-1}$, which was the same magnitude as other oligotrophic oceans. Indirect evidence from benthic studies, however, indicates that organic fluxes are enhanced on the crest and southern flank of the Chatham Rise (Probert and McKnight, 1993; Nodder et al., 2003). It is thus clear that information on the spatial variation of POC export is mandatory if we are to evaluate whether the enhanced primary production in the frontal zone also leads to enhanced export production.

In the present study, we utilized a particle-reactive radionuclide ^{234}Th ($t_{1/2}$ = 24.1 d) as a tracer for particle export from the upper ocean. The technique has been applied widely in many oceanographic settings to examine processes occurring on time-scales of days to weeks (e.g. Coale and Bruland, 1985, 1987; Buesseler, 1992, 1998; Cochran and Masque, 2003; Dai and Benitez-Nelson, 2001; Waples et al., 2006). A further technological advantage is the use of the recently developed small volume technique that enables high resolution sampling (Benitez-Nelson et al., 2001a; Buesseler et al., 2001a; Cai et al., 2006a), which is essential in order to capture the variability of the particle dynamics and export fluxes in regions, such as the STF, that are characterized by dynamic hydrography (Cai et al., 2008; Buesseler et al., 2009). Indeed, with high resolution sampling, Cai et al. (2008) observed significant variations of ^{234}Th deficit in the South China Sea, with enhanced Th and POC fluxes along the western and southern boundaries. Buesseler et al. (2009) also discovered high spatial variability in the northern subtropical gyre at ALOHA station off Hawaii, where it was expected there would be a homogenous distribution of POC flux from the surface ocean.

The present study aims to examine the spatial distribution, magnitude and variability of upper ocean POC export in the STF area over the Chatham Rise to the east of New

BGD
8, 9535–9576, 2011

Zealand by using high spatial resolution sampling of ^{234}Th concentrations. We show that ^{234}Th-based POC export is not significantly enhanced in the frontal zone, despite high chlorophyll levels compared to the adjacent SAW and STW.

2 Methods

2.1 Sample collection

Samples were collected in late austral autumn-early winter from 23 May to 12 June in 2008 on board R/V *Tangaroa*, operated by the National Institute of Water and Atmospheric Research (NIWA) Ltd, New Zealand (NIWA voyage TAN0806). High spatial resolution sampling at 23 stations, covering a surface area of about 25 000 km^2, was conducted during the cruise (Fig. 1). Water samples were collected using 10 l Niskin bottles mounted onto a rosette sampler attached to a Seabird SBE9/11plus conductivity-temperature-depth (CTD) sensor. A sub-sample of 4 l seawater was used to determine the total ^{234}Th activity (see below) and another 8 l was filtered onto a 25-mm diameter Quartz Microfiber (QMA, norminal pore size ~1.0 µm) for particulate ^{234}Th and POC measurements. Samples were collected at 5 depths in the upper 100 m (normally 10, 20, 50, 70, and 100 m), except along transect *M* where sampling was conducted at a finer depth resolution throughout the water column to better define the vertical structure of ^{234}Th over the Chatham Rise (shown as a blue line on Fig. 1). Since this was the first ^{234}Th study over the Chatham Rise, such an intensive sampling strategy enabled a robust description of both the vertical and spatial distribution of ^{234}Th.

2.2 ^{234}Th analysis

We used the small-volume MnO_2 co-precipitation technique for our total ^{234}Th analysis, as initially developed by Benitez-Nelson et al. (2001a) and Buesseler et al. (2001a), and further modified by Cai et al. (2006a). Four litre seawater samples were immediately

BGD
8, 9535–9576, 2011

acidified with 6 ml concentrated HNO_3 and spiked with ~10 dpm ^{230}Th after collection. The samples were then mixed vigorously and allowed to stand for 12 h for isotopic equilibration. The pH was then brought up to 8.00–8.20 and thorium isotopes were co-precipitated with MnO_2 by adding 0.25 ml $KMnO_4$ (3.0 g l^{-1}) and 0.25 ml $MnCl_2$ (8.0 g $MnCl_2 \bullet 4H_2O$ l^{-1}). The formation of the MnO_2 precipitate was accelerated by heating to approximately 90 °C in a water bath for 2 h. The precipitate was then filtered on a 25 mm QMA filter after samples were cooled to room temperature. The QMA filter was baked at about 100–200 °C until dryness, and the filter was then mounted under a layer of Mylar and two layers of aluminum foil (total density ~7.2 mg m^{-2}) for beta-counting at sea by a gas-flow proportional low-level RISØ beta counter (Model GM-25-5, RISØ National Laboratory). These samples were re-counted for background levels 6 months after the cruise (i.e. >5 half-lives of ^{234}Th).

The QMA filter used for particulate ^{234}Th determination was dried at 50 °C in an oven for 24 h, and then mounted and beta-counted as above for the total ^{234}Th sample. The average background levels for total and particulate ^{234}Th were 0.45 and 0.32 counts per minute (cpm), respectively.

We used an alpha spectrometric method for our total ^{234}Th recovery analysis (Cai et al., 2006a). Samples were demounted after background counting, spiked with ~10 dpm ^{228}Th (^{232}U-^{228}Th solution) and then digested by adding 10 ml concentrated HNO_3, 1 ml HF and 1 ml H_2O_2. Thorium isotopes were purified through iron precipitation and classic anion column. Elutents were then evaporated onto a 25 mm stainless steel disc after extraction using 1.5 ml of 0.25 mol l^{-1} theonyl trifluoroacetone(TTA)/benzene solution. The disc was counted by alpha spectrometry (Octete^{TM} PC) until both thorium isotopes (^{230}Th and ^{228}Th) reached more than 2500 counts. Most of final recoveries for ^{230}Th were between 80 % and 103 %. The average of the recoveries was 90.2 ± 1.4 % (mean ± 1 standard deviation).

Instead of undertaking specific sample analyses, we used the relationship: A_U (dpm l^{-1}) = 0.07081 × salinity to estimate the ^{238}U activity (A_U) in the seawater according to Chen et al. (1986).

BGD
8, 9535–9576, 2011

2.3 POC and Particulate Nitrogen (PN) analysis

After beta-counting for particulate ^{234}Th, the samples were demounted for POC and PN analysis. The filters were placed in Petri dishes and fumed using concentrated hydrochloric acid for 24 h to remove the carbonate phase. POC concentrations were then determined by a PE-2400 SERIES II CHNS/O analyzer, according to the JGOFS protocols (Knap et al., 1996). Replicate procedural C blanks from sampling to instrumental carbon determination have been tested before (Chen, 2008), and were all less than 6 µg C and 2 µg N, which typically accounted for less than 10 % of the sample POC and PN, respectively. The precision for our POC measurements were all better than 10 % (Cai et al., 2006a; Chen, 2008).

2.4 Other ancillary parameters

The temperature and salinity vertical profile data were all obtained from a Seabird SBE9/11plus CTD. A Wetlabs fluorometer, interfaced with the CTD, was used to determine the fluorescence at an excitation and emission wavelength of 470 and 695 nm.

3 Results

3.1 Hydrography

The complex hydrological characteristics of the STF are displayed by the relationship between potential temperature and salinity in Fig. 2. In the upper ocean, distinctive differences of water characteristics were found at all stations, representing different degrees of mixing. The surface temperature and salinity changed dramatically over the sampled area from lows of 9.4 °C and 34.2, respectively, in surface waters with SAW affinities, to highs of 15.2 °C and 35.2 to those waters associated with STW.

Figure 3 shows the spatial distributions of temperature and salinity at 2 m and 100 m water depths. The gradients of salinity and temperature were much greater in the

BGD
8, 9535–9576, 2011

region between 43° S and 44° S, coinciding with the crest and upper southern flank of the Chatham Rise. Vertically, the upper ocean was well-stratified at all stations sampled in the STF (Fig. 4a, b, and c). However, the depth of the surface isothermal mixed-layer, defined by using a criterion based on the density with 0.5 °C of temperature difference from the reference depth (Kara et al., 2000), was not uniform between stations, ranging from 54 m to 178 m. Typically and as illustrated in Fig. 4, depth of the mixed-layer at high salinity stations was higher than at mid- and low salinity ones (see next section for definitions of water types).

3.2 Fluorescence and POC distribution

Fluorescence intensity collected from the CTD was calibrated during the cruise (Chlorophyll-a = 0.639× Fluorescence, R^2 = 0.87, n = 50), and is used here as an effective tracer for chlorophyll-a concentration. Fluorescence ranged from the background value of 0.06 to 2.2. Vertically, fluorescence was highest and homogenously distributed within the surface mixed-layer. Below the mixed-layer, the fluorescence level began to drop reaching background, effectively zero levels (Fig. 4a, b). Regionally, the average fluorescence in the upper 100 m varied from 0.39 to 0.98, with an average of 0.58 where S was greater than 34.8, as illustrated in Fig. 6d. Fluorescence increased in surface waters at S = 34.8 until it reached the maximum of 2.43 at S = 34.5. The average value of fluorescence between S = 34.8 and S = 34.5 was as high as 1.24. At S < 34.5, the fluorescence level began to drop until it stabilized at ~0.6 when S was less than 34.3. For the ease of discussion, we divided the STF waters of our study area into three parts: low (S < 34.8), mid- (34.5 < S < 34.8) and high salinity (S > 34.8), according to the vertical and horizontal distribution of fluorescence from the CTD casts.

POC concentrations varied from 0.4 µmol C l^{-1} to 6.1 µmol C l^{-1} across the study area (Table 1). In the upper mixed-layer, POC distributions generally followed that of fluorescence, indicating its relationship with phytoplankton biomass. Regionally, POC concentration was also enhanced in mid-salinity waters. The average POC concentration in the upper 100 m was 3.92 µmol C l^{-1} in mid-salinity waters, compared to

BGD
8, 9535–9576, 2011

2.39 µmol C l^{-1} and 2.58 µmol C l^{-1} in high and low salinity waters, respectively. In a departure from the vertical distribution of fluorescence, POC concentrations were often higher near the bottom of the water column, which may be indicative of the near-bottom sediment re-suspension (e.g. Nodder, 1997; Nodder et al., 2007).

The C/N ratio was quite stable in the upper ocean, ranging from 5.2 to 8.5, with an average of 6.6 ± 1.5 (n = 146), which is almost identical to the Redfield ratio of 6.63 (Redfield et al., 1963). No obvious changes in C/N ratio were found in association with changes in salinity, suggesting that the particles in the study area were predominantly biogenic in origin.

3.3 ^{234}Th distribution

3.3.1 Vertical profiles of ^{234}Th

Particulate and total ^{234}Th activities are listed in Table 1. Profiles of three selected stations from low, mid- and high salinity waters are shown in Fig. 4. The activities of total ^{234}Th varied from 1.42 ± 0.092 dpm l^{-1} to 2.54 ± 0.14 dpm l^{-1}. Particulate ^{234}Th activities on suspended particles were variable, varying from 0.10 ± 0.01 dpm l^{-1} to 0.70 ± 0.02 dpm l^{-1}. The ^{234}Th activity profile in the upper 100 m was related to the vertical distribution of fluorescence. As illustrated in Fig. 4, total ^{234}Th was homogenously distributed within the isothermal mixed-layer, with activities lower than for soluble ^{238}U. Below the mixed-layer, the activity of total ^{234}Th began to increase as the fluorescence leveled off, until it reached secular equilibrium with ^{238}U at the base of the euphotic zone (Ez) where fluorescence reached its minimum. At stations with depths of Ez greater than 100 m, the total ^{234}Th activity was in deficit with respect to ^{238}U from 0–100 m. The vertical distribution of particulate ^{234}Th also generally resembled that of fluorescence and POC, in that its activity was homogenous within and decreased below the mixed-layer. Not surprisingly, higher particulate ^{234}Th activities were related to higher levels of fluorescence, indicating intensive scavenging of biogenic particles in high chlorophyll-a waters. However, total ^{234}Th activities seemed to be independent of

BGD
8, 9535–9576, 2011

fluorescence and/or biomass. As shown in Fig. 4, the fluorescence level at mid-salinity station C15 was two times higher than the low salinity station C17, but the activities of total ^{234}Th were similar at both stations.

3.3.2 Meridional distribution of ^{234}Th

To better describe the spatial distribution pattern of ^{234}Th in the STF across the Chatham Rise, transect *M*, consisting of stations C5, C6, C7, C17, C18, and C20, was sampled throughout the water column (shown in Fig. 5). Generally, total ^{234}Th was in deficit in upper and near-bottom waters, and was in equilibrium with ^{238}U over the mid-water column. No meridional trends were found in the upper water column along transect *M*. Particulate ^{234}Th was higher within the Ez and in bottom waters than in the mid-water column. Interestingly, at mid-depths of 300–600 m, a deficit of total ^{234}Th was found in waters on both sides of the Chatham Rise crest. This observation may reflect the horizontal transport of the re-suspended particles along the Chatham Rise flanks, consistent with the near-bottom increases in particle fluxes from sediment trap (Nodder, 1997; Nodder and Northcote, 2001) and benthic studies (Nodder et al., 2007) in this area.

3.3.3 Regional distribution of ^{234}Th

To provide a composite view of the regional distribution of ^{234}Th in relationship to different water types, the total and particulate ^{234}Th activities are superimposed on a T/S diagram (Fig. 6). Similar to fluorescence and POC, the activities of particulate ^{234}Th in the upper ocean were enhanced in mid-salinity waters, where the average of particulate ^{234}Th activities increased up to 0.45 ± 0.01 dpm l^{-1}, which was two times higher than in the high salinity waters (0.20 ± 0.01 dpm l^{-1}). Noticeably, however, high activities of particulate ^{234}Th were not necessarily correlated with low total ^{234}Th activities. Such a distribution pattern was also true for total ^{234}Th among the three water types. The activities of total ^{234}Th in mid-salinity waters varied from 1.44 ± 0.18 dpm l^{-1}

BGD
8, 9535–9576, 2011

to 2.41 ± 0.08 dpm l^{-1}, with an average of 1.97 ± 0.10 dpm l^{-1}, and similarly from 1.42 ± 0.09 dpm l^{-1} to 2.47 ± 0.08 dpm l^{-1} in the high salinity waters, with an average of 1.88 ± 0.10 dpm l^{-1}. In comparison, total ^{234}Th activity ranged from 1.61 ± 0.06 to 2.34 ± 0.08 dpm l^{-1} in low salinity waters, with an average of 1.93 ± 0.10 dpm l^{-1}.

3.4 ^{234}Th export flux estimates

The export flux of ^{234}Th at a specific depth horizon can be estimated by using the following equation:

$$\frac{\delta A_{\mathrm{Th}}}{\delta t} = A_{\mathrm{U}}\lambda_{\mathrm{Th}} - A_{\mathrm{Th}}\lambda_{\mathrm{Th}} - P + V \quad (1)$$

where $\frac{\delta A_{\mathrm{Th}}}{\delta t}$ is the rate of change of total ^{234}Th activity, A_{U} is the ^{238}U activity estimated from the U-S relationship (Chen et al., 1986), A_{Th} is the total ^{234}Th activity, λ_{Th} is the decay constant for ^{234}Th (0.02876 d^{-1}), P is the net removal flux of ^{234}Th on particles, and V is the sum of contributions from advection and diffusion.

The Steady State (SS) model is applicable when little temporal change ($\frac{\delta A_{\mathrm{Th}}}{\delta t}$) occurs in ^{234}Th activities or SS ^{234}Th flux is low (Savoye et al., 2006). However, when there are rapid changes in ^{234}Th activities, for example, during the algal bloom period or within physically dynamic regions, such as the STF, a non-steady state (NSS) ^{234}Th flux model is necessary (Buesseler et al., 1992). To implement a NSS ^{234}Th flux model, however, time-series observations for the same water mass are needed. In a practical sense, since there are difficulties in tracing specific water masses in the ocean, most studies have adopted a protocol to visit the same station at least two times during a particular study period (Benitez-Nelson et al., 2001b; Coppola et al., 2005; Kawakami and Honda, 2007). NSS ^{234}Th flux can then be calculated by using following equation (Buesseler et al., 1992):

$$P_{\mathrm{NSS}} = \frac{\lambda(P_{\mathrm{SS-2}} - P_{\mathrm{SS-1}}e^{-\lambda t})}{1 - e^{-\lambda t}} \quad (2)$$

BGD
8, 9535–9576, 2011

where P_{NSS} is the NSS ^{234}Th export flux, and P_{SS-1} and P_{SS-2} are the SS ^{234}Th flux during the first and second visit, respectively. During our voyage, two stations (C3 and C4) were visited twice. The profiles of the temperature, salinity and ^{234}Th activity for these stations are shown in Fig. 7. At C3, differences in temperature and salinity of the upper 100 m between the two visits were 0.5 °C and 0.02, respectively. In contrast, at C4, larger differences were found: 2.1 °C for temperature and 0.37 for salinity, which clearly indicated different water masses were present at this location between the two visits. Due to the relatively minor changes in hydrography, we assume the same water mass was sampled during the two visits at C3. Given the potential influence from the bottom re-suspension at this shallow station (see later), NSS ^{234}Th flux from the upper 10 m is calculated as 247 dpm m^{-2} d^{-1}. The SS ^{234}Th fluxes from the upper 10 m for the two visits to C3 were 242 and 244 dpm m^{-2} d^{-1}, so that, there is obviously little temporal variation of ^{234}Th flux at this location. As such, the SS model is regarded to be mostly suitable for our ^{234}Th fluxes calculations at all the other locations in the STF.

Physical processes may also influence the estimation of downward ^{234}Th fluxes. Previous studies indicate that currents over the Chatham Rise can be strong, but variable, with alternating zones of convergence and divergence, although net zonal flows dominate along the northern and southern edges of Chatham Rise and predominantly meridional flows occur over the rise itself (Chiswell, 1996; Sutton, 2001). Given the little change in total ^{234}Th activities along the salinity gradients (as shown in Fig. 6), however, we assume that the horizontal contribution to the ^{234}Th fluxes is small compared to the downward vertical component of ^{234}Th export. Therefore, the V term in Eq. (3) is neglected in our ^{234}Th fluxes estimates.

Based on the above discussion, the P term in Eq. (1) can then be solved as follows:

$$P = \lambda_{Th}(A_U - A_{Th}) \quad (3)$$

BGD
8, 9535–9576, 2011

In our case, the steady state (SS) downward flux of total ^{234}Th from the depth horizon of 100 m can be integrated by:

$$P = \lambda_{Th} \int_0^{100} (A_U - A_{Th}) dz \quad (4)$$

The calculated ^{234}Th flux results for the upper 100 m of the water column are listed in Table 2. SS ^{234}Th fluxes range from 991 ± 263 dpm m^{-2} d^{-1} to a maximum of 2627 ± 239 dpm m^{-2} d^{-1}, with an average of 1574 ± 974 dpm m^{-2} d^{-1} ($n = 25$). It should been noted that the highest value is from Station C3 with a bottom depth of 125 m, and which consequently may be influenced by near-bottom re-suspension. As discussed previously, we also separate our ^{234}Th flux data into three groups. In low salinity waters, SS ^{234}Th fluxes varied from 1015 ± 237 dpm m^{-2} d^{-1} to 1592 ± 142 dpm m^{-2} d^{-1}, with an average of 1304 ± 92 dpm m^{-2} d^{-1} ($n = 3$). In mid-salinity waters, the flux varied from 991 ± 263 dpm m^{-2} d^{-1} to 1862 ± 136 dpm m^{-2} d^{-1}, with an average of 1484 ± 86 dpm m^{-2} d^{-1} ($n = 9$). In high salinity waters, SS ^{234}Th fluxes were similar to those in mid-salinity waters, namely, 1104 ± 150 dpm m^{-2} d^{-1} to 2627 ± 239 dpm m^{-2} d^{-1}, with an average of 1761 ± 46 dpm m^{-2} d^{-1} ($n = 13$).

3.5 Bottle POC/^{234}Th ratios

Bottle POC/^{234}Th ratios are all listed in Table 1. This ratio was quite variable, ranging from 2.6 µmol C dpm^{-1} to 28.7 µmol C dpm^{-1}. All POC/^{234}Th ratios were separated into three groups according to the salinity, as shown in Fig. 8. Consistent with many prior studies, POC/^{234}Th was higher and more variable in the upper ocean, compared to those in the deep ocean (Buesseler et al., 2006). Interestingly, it was generally lower in mid- and low salinity waters than in high salinity waters, reflecting different biological effects on carbon and thorium. This difference disappeared at and below 100 m. At the export horizon of 100 m, bottle POC/^{234}Th ratios varied from 4.4 ± 0.3 µmol C dpm^{-1} to 13.7 ± 1.1 µmol C dpm^{-1}, with an average of 7.7 ± 3.5 µmol C dpm^{-1} (Table 2). Similar to ^{234}Th fluxes, no difference in POC/^{234}Th ratio was found among the three water

BGD
8, 9535–9576, 2011

types. In high salinity waters, POC/^{234}Th ratio ranged from 4.4 ± 0.3 µmol C dpm^{-1} to 13.6 ± 1.1 µmol C dpm^{-1}, with an average of 8.0 ± 2.4 µmol C dpm^{-1}. In mid-salinity waters, it varied from 5.1 ± 0.4 µmol C dpm^{-1} to 11.0 ± 1.0 µmol C dpm^{-1}, with an average of 7.3 ± 2.6 µmol C dpm^{-1}, and similarly in low salinity waters, it was less variable, ranging from 6.4 ± 0.4 µmol C dpm^{-1} to 6.6 ± 0.4 µmol C dpm^{-1}, with an average of 6.5 ± 0.4 µmol C dpm^{-1}.

4 Discussion

4.1 POC/^{234}Th ratios and POC export flux

POC export fluxes can be estimated by multiplying ^{234}Th fluxes by POC/^{234}Th ratios of sinking particles (Buesseler et al., 1992). To better constrain the POC export from the upper ocean using the ^{234}Th method, knowledge of POC/^{234}Th in sinking particles should be examined. However, in the present study, only bottle POC/^{234}Th was collected during the cruise.

Many studies have shown that the bottle POC/^{234}Th ratio is typically higher than in pump and trap samples (Buesseler et al., 2006; Cai et al., 2008; Kawakami and Honda, 2007). Although bottle POC/^{234}Th ratios from particles in bottle samples are not expected to be particularly representative of sinking particles, it is reasonable to apply these measurements as an upper limit for the true sinking POC/^{234}Th ratio (Cai et al., 2008). Another advantage is that bottle filtrations enabled us to undertake high spatial resolution sampling of POC/^{234}Th, compared to the spatially limited deployment of in situ pumps and sediment traps.

The POC export fluxes estimated from SS ^{234}Th flux and bottle POC/^{234}Th at the depth horizon of 100 m are listed in Table 2. POC export ranged from 5.6 ± 0.7 to 29.8 ± 2.4 mmol C m^{-2} d^{-1}, with an average of 12.2 ± 0.4 mmol C m^{-2} d^{-1} ($n = 25$). As expected, POC export fluxes were similar among all three water types, which is in good agreement with the ^{234}Th flux distribution. POC flux varied from 5.6 ± 0.7 mmol C

BGD
8, 9535–9576, 2011

$m^{-2}\,d^{-1}$ to 29.8 ± 2.4 mmol C $m^{-2}\,d^{-1}$ in high salinity waters, with an average of 14.1 ± 0.6 mmol C $m^{-2}\,d^{-1}$ ($n = 13$), and from 6.7 ± 1.1 mmol C $m^{-2}\,d^{-1}$ to 10.4 ± 1.1 mmol C $m^{-2}\,d^{-1}$ in low salinity water, with an average of 8.5 ± 0.3 mmol C $m^{-2}\,d^{-1}$ ($n = 3$). In comparison, POC flux ranged from 6.0 ± 1.0 mmol C $m^{-2}\,d^{-1}$ to 16.1 ± 1.6 mmol C $m^{-2}\,d^{-1}$ in mid-salinity waters, with an average of 10.6 ± 0.4 mmol C $m^{-2}\,d^{-1}$ ($n = 9$).

Due to the lack of an effective methodology for determining downward POC export in such a physically dynamic area, few similar studies have been carried out in STF over Chatham Rise or even in other STF areas globally. Nodder (1997) attempted to test the hypothesis that STF is a region of elevated export production in austral autumn via the deployment of a free-floating, surface-tethered, cylindrical sediment trap array on the northern side of the STF over the Chatham Rise. Mean particulate carbon fluxes were estimated to be ~2.5 mmol C $m^{-2}\,d^{-1}$ at 200 m water depth, which is similar in magnitude to other locations in oligotrophic waters. Nodder and Alexander (1998) showed that spring particulate phosphorus fluxes at ~100 m in the STF were almost double those in winter 1993, These earlier studies, however, were limited in their spatial coverage, which restricts the reliability of these results when extrapolated to a more regional basis to cover the entire STF. Long-term moored sediment traps were deployed for a year at 300 m and 1000 m in the STF on the flanks of the Chatham Rise to investigate the seasonal variation of particle fluxes (Nodder and Northcote, 2001). POC export reached its maximum in spring (14.8 mmol C $m^{-2}\,d^{-1}$ at 300 m in the north and 4.8 mmol C $m^{-2}\,d^{-1}$ in the south), and annual average POC fluxes were calculated to be 10.1 mmol C $m^{-2}\,d^{-1}$ in the north, compared to 4.1 mmol C $m^{-2}\,d^{-1}$ in the south. POC export was also determined in frontal zones (including the STF and Polar Front) in Indian Ocean sector of Southern Ocean in summer using the ^{234}Th method (Coppola et al., 2005). At an export depth horizon of 100 m, POC export varied from 0.1 to 2.5 mmol C $m^{-2}\,d^{-1}$, which is very low compared to other observations in the Southern Ocean (Buesseler et al., 2001b; Rutgers van der Loeff et al., 1997, 2002; Trull et al., 2001). The low diatom dominance in the water column was hypothesized to result in these low export fluxes. However, direct comparisons between these studies

BGD
8, 9535–9576, 2011

are difficult due to differences in the regional oceanography, observation duration, the chosen export depth horizon and methodologies.

The export fluxes presented here for the STF on the Chatham Rise, are also only applicable to the season in which they were collected (i.e. late autumn-early winter), and it is expected that POC fluxes in the highly productive spring might be significantly enhanced in comparison (Nodder and Alexander, 1998; Nodder and Northcote, 2001). Nevertheless, the calculated POC fluxes using the ^{234}Th method are at least similar in magnitude to previous measurements of POC export in the same area, and provide us with the first appreciation of the substantial degree of spatial variability that could be expected in POC flux to the seafloor on the Chatham Rise. The POC flux estimated at 100 m in the present study decreased from west to east and from north to south across the rise (Fig. 9d). Benthic biomass and activity is generally higher on the southern flank of the Chatham Rise, compared to the crest and northern flank (Nodder et al., 2003, 2007; Probert and McKnight, 1993), which is somewhat incongruous with the lower POC fluxes suggested by this study and previous sediment trap results (Nodder and Northcote, 2001). Thus, it is likely that it is the quality, rather than the quantity, of POC supply to the benthos that has the most influence in structuring seafloor communities in this region (Nodder et al., 2003, 2007).

4.2 Comparison between low, mid- and high salinity waters showing insignificant export production enhancement in the STF

As shown in the Results section, all fluorescence, POC and particulate ^{234}Th data suggest enhanced biological particle production in the upper 100 m of mid-salinity waters, compared to low and high salinity waters within the STF. This trend continues to hold if we integrate all of these data from surface to 100 m (Table 2). The average inventories of fluorescence, POC and particulate ^{234}Th of 124.7 m^{-2}, 3.92 mol C m^{-2}, and $(4.5 \pm 0.1) \times 10^4$ dpm m^{-2}, respectively, in mid-salinity waters, were again high, compared to 57.7 m^{-2}, 2.48 mol C m^{-2}, and $(2.00 \pm 0.1) \times 10^4$ dpm m^{-2} in high salinity

BGD
8, 9535–9576, 2011

waters and 57.4 m^{-2}, 2.58 mol C m^{-2}, and $(3.46 \pm 0.1) \times 10^4$ dpm m^{-2} in low salinity waters. T-tests with unequal variance were carried out to compare the differences between the mid- and high salinity waters showed that P values ($\alpha = 0.05$) for fluorescence, POC and particulate ^{234}Th were 0.003, 0.002, and 0.000014, respectively (Table 3), and P values would be 0.005, 0.02, and 0.03 for the comparison between mid- and low salinity waters. Such analyses indicate that the mid-salinity waters were statistically different from the other two water types. Note that the biological enhancement observed in the mid-salinity waters was also observed for PP measured in a parallel study on the same cruise (Jill Schwarz, NIWA, personal communication). It is interesting that the enhancement of particulate ^{234}Th in mid-salinity waters was much stronger than for fluorescence and POC.

The high chlorophyll-*a* biomass and/or PP levels in the STF have been well-defined in previous studies. For example, phytoplankton biomass in winter and spring were 4 and 6 times higher, respectively, in the STF than the adjacent low salinity SAW (Hall et al., 1999). The mean PP rate in winter could be as high as 22 mmol C m^{-2} d^{-1}, which was 4 times higher than that in SAW (Bradford-Grieve et al., 1999). Remote-sensing satellite data also show that the STF is characterized by the year-around heightened pigment concentrations (Comiso et al., 1993; Murphy et al., 2001).

Moreover, studies have proposed that the elevated iron levels caused by mixing induced by the shallow bathymetry of Chatham Rise and/or the atmospheric deposition from Australian dust may have led to such high biomass/PP levels, a process frequently termed "natural iron fertilization". Indeed, Boyd et al. (2004) determined the dissolved iron concentrations and potential sources in a transect across the STF. Dissolved iron concentrations in frontal surface waters reached the highest values of 0.8 nmol l^{-1} at about 43° S, which is coincident geographically with the crest of the Chatham Rise. Note that iron concentrations dropped dramatically to less than 0.2 nmol l^{-1} within 1 degree of latitude to the north.

In contrast to the enhancement of primary production within the STF, little difference in POC and ^{234}Th fluxes were found among the three water types identified in

BGD
8, 9535–9576, 2011

the present study. A t-test comparing the POC and ^{234}Th fluxes at the 100 m export horizon between high and mid-salinity waters resulted in P values ($\alpha = 0.05$) of 0.097 and 0.100, respectively (Table 3). The same parameters were compared between the mid- and low salinity waters, similar results were also shown (see Table 3). These relationship still held when all parameters were integrated to the bottom of Ez (instead to a fixed depth), which is not surprising given the fact that sinking particles originate mainly within the Ez and shallow remineralization has frequently been found just below the Ez (e.g. Buesseler and Boyd, 2009). Thus, the differences in POC and ^{234}Th fluxes 100 m and/or the base of Ez among the three water types were indistinguishable.

The reason why the elevated PP levels in the STF frontal zone, especially in our mid-salinity waters, did not lead to an increase in POC export is still unclear. There are several aspects that may induce relative low POC export. The most obvious one is related to the planktonic community structure, which has been regarded as one of the major drivers determining downward particle flux characteristics (Boyd and Newton, 1995; Michaels and Silver, 1988). Although we do not have community structure data from the present study, previous research has suggested that the STF is characterized by abundant diatoms (Boyd et al., 1999; Bradford-Grieve et al., 1997), which would have favored higher POC export. Alternatively, bacteria may remineralize POC before it sinks down to depth, thereby negating the high PP at the surface. The ratio between bacterial production and PP has been measured in the STF as 5–47 %, compared to 14–178 % in STW and SAW (Hall et al., 1999), suggesting that such low bacterial production would not be expected to significantly affect POC export in the frontal zone. In the context of the above reasoning, the most likely reason for the reduction in POC export in the STF is zooplankton grazing. Indeed, Hall et al. (1999) demonstrated that >78 % of daily PP can be grazed by microzooplankton in the STF in austral spring and winter. In contrast, mesozooplankton grazing is likely to be in the order of only 1–2 % of daily PP (Bradford-Grieve et al., 1998). Unlike mesozooplanton, the fecal pellets produced by microzooplankton are smaller and easily remineralized in the upper ocean and may not contribute significantly to export flux (Boyd and Newton, 1995; Michaels

BGD
8, 9535–9576, 2011

and Silver, 1988), as also suggested by other studies in the STF region (Nodder and Gall, 1998; Zeldis et al., 2002).

5 Conclusions

The present study applied a high resolution ^{234}Th sampling technique to define the magnitude and distribution of POC export in the STF region, which revealed with greater confidence that the POC export fluxes were on the order of 5.6 ± 0.7 to 29.8 ± 2.4 mmol C $m^{-2}\,d^{-1}$, with an overall average of 12.2 ± 0.4 mmol C $m^{-2}\,d^{-1}$ ($n = 25$). There was little spatial variation among the low, mid- and high salinity waters, despite differences in biological particle production, as inferred from fluorescence/chlorophyll-*a* profiles. The present study, on the other hand, confirmed that the STF region is characterized by elevated PP, in particular, in the mid- salinity waters ($34.5 < S < 34.8$), presumably stimulated by so-called natural iron fertilization processes (Boyd et al., 1999, 2004; Pollard et al., 2009).

The present study, therefore, implies that natural iron fertilization does not necessarily lead to the enhancement of POC export in STF regions. It must be pointed out that, compared to other natural/artificial iron experiments (Boyd et al., 2007), the present study was carried out in a different season (late autumn-early winter cf. summer) and latitude (43–44° cf. >50–60°). Therefore, we can anticipate that differences in temperature, latitude, season and region will induce different ecosystem responses.

Acknowledgements. This study was funded by the Foundation of Science, Research and Technology (New Zealand) via the Coasts and Oceans Outcome-Based Investment (C01X0501). KZ was supported by a NIWA Capability Fund Visiting Scientist grant for him to participate in the voyage. The preparation of the manuscript was supported by the National Natural Science Foundation of China through grant NSFC 40821063 to MHD. We thank the Captain, officers and crew of R/V *Tangaroa* for their assistance in sample collection during voyage TAN0806, as well as other voyage participants, especially Steve George for operating the CTD. We also thank Pinghe Cai and Ken Buesseler for their constructive comments on the early stage of this paper.

BGD
8, 9535–9576, 2011

References

Bacon, M. P., Cochran, J. K., Hirschberg, D., Hammar, T. R., and Fleer, A. P.: Export flux of carbon at the equator during the EqPac time-series cruises estimated from ^{234}Th measurements, Deep Sea Res. II, 43, 1133–1153, 1996.

Behrenfeld, M. J. and Falkowski, P. G.: A consumer's guide to phytoplankton primary productivity models, Limnol. Oceanogr., 42, 1479–1491, 1997.

Benitez-Nelson, C. R., Buesseler, K. O., Karl, D. M., and Andrews, J.: A time-series study of particulate matter export in the North Pacific Subtropical Gyre based on ^{234}Th:^{238}U disequilibrium, Deep Sea Res. I, 48, 2595–2611, 2001a.

Benitez-Nelson, C. R., Buesseler, K. O., Van der Loeff, M. R., Andrews, J., Ball, L., Crossin, G., and Charette, M. A.: Testing a new small-volume technique for determining ^{234}Th in seawater, J. Radioanal. Nucl. Chem., 248, 795–799, 2001b.

Boyd, P. and Newton, P.: Evidence of the potential influence of planktonic community structure on the interannual variablity of particulate organic carbon flux, Deep Sea Res. I, 42, 619–639, 1995.

Boyd, P., LaRoche, J., Gall, M., Frew, R., and McKay, R. M. L.: Role of iron, light, and silicate in controlling algal biomass in subantarctic waters SE of New Zealand, J. Geophys. Res., Oceans, 104, 13395–13408, 1999.

Boyd, P., McTainsh, W. G., Sherlock, V., Richardson, K., Nichol, S., Ellwood, S., and Frew, R.: Episodic enhancement of phytoplankton stocks in New Zealand subantarctic waters: Contribution of atmospheric and oceanic iron supply, Global Biogeochem. Cy., 18, GB1029, doi:1029/2002GB002020, 2004.

Boyd, P., Jickells, T. D., Law, C. S., Blain, S., Boyle, E. A., Buesseler, K. O., Coale, K. H., Cullen, J. J., de Baar, H. J. W., Follows, M., Harvey, M., Lancelot, C., Levasseur, M., Owens, N. P. J., Pollard, R. T., Rivkin, R. S., Sarmiento, J., Schoemann, V., Smetacek, V., Takeda, S., Tsuda, A., Turner, S., and Watson, A. J.: Mesoscale Iron Enrichment Experiments 1993–2005: Synthesis and Future Directions, Science, 315, 612–617, 2007.

Bradford-Grieve, J., Murdoch, R., James, R., Oliver, R., and McLeod, R.: Mesozooplankton biomass, composition, and potential grazing pressure on phytoplankton during austral winter and spring 1993 in the Subtropical Convergence region near New Zealand, Deep Sea Res. I, 45, 1709–1737, 1998.

Bradford-Grieve, J. M., Chang, F. H., Gall, M., Pickmere, S., and Richards, F.: Size-fractionated

BGD
8, 9535–9576, 2011

phytoplanton standing stocks and primary production during austral winter and spring 1993 in Subtropical Convergence region near New Zealand., N. Z. J. Mar. Freshwater Res., 31, 201–224, 1997.

Bradford-Grieve, J. M., Boyd, P. W., Chang, F. H., Chiswell, S., Hadfield, M., Hall, J. A., James, M. R., Nodder, S. D., and Shushkina, E. A.: Pelagic ecosystem structure and functioning in the Subtropical Front region east of New Zealand in austral winter and spring 1993, J. Plankton Res., 21, 405–428, 1999.

Buesseler, K. O. and Boyd, P. W.: Shedding light on processes that control particle export and flux attenuation in the twilight zone of the open ocean, Limnol. Oceanogr., 54, 1210–1232, 2009.

Buesseler, K. O., Bacon, M. P., Cochran, J. K., and Livingston, H. D.: Carbon and nitrogen export during the JGOFS North Atlantic bloom experiment estimated from ^{234}Th:^{238}U disequilibria, Deep Sea Res., 1115–1137, 1992.

Buesseler, K. O, Ball, L., Andrews, J., Benitez-Nelson, C., Belastock, R., Chai, F., and Chao, Y.: Upper ocean export of particulate organic carbon in the Arabian Sea derived from thorium-234, Deep Sea Res. II, 45, 2461–2487, 1998.

Buesseler, K. O., Ball, L., Andrews, J., Cochran, J. K., Hirschberg, D. J., Bacon, M. P., Fleer, A. P., and Brzezinski, M. A.: Upper ocean export of particulate organic carbon and biogenic silica in the Southern Ocean along 170° W, Deep Sea Res. II, 48, 4275–4297, 2001a.

Buesseler K. O., Benitez-Nelson, C. R., van der Loeff, M. R., Andrews, J., Ball, L., Crossin, G., and Charette, M. A.: An intercomparison of small- and large-volume techniques for thorium-234 in seawater, Mar. Chem., 74, 15–28, 2001b.

Buesseler, K. O., Benitez-Nelson, C. R., Moran, S. B., Burd, A., Charette, M., Cochran, J. K., Coppola, L., Fisher, N. S., Fowler, S. W., Gardner, W., Guo, L. D., Gustafsson, O., Lamborg, C., Masque, P., Miquel, J. C., Passow, U., Santschi, P. H., Savoye, N., Stewart, G., and Trull, T.: An assessment of particulate organic carbon to thorium-234 ratios in the ocean and their impact on the application of ^{234}Th as a POC flux proxy, Mar. Chem., 100, 213–233, 2006.

Buesseler, K. O., Lamborg, C., Cai, P., Escoube, R., Johnson, R., Pike, S., Masque, P., McGillicuddy, D., and Verdeny, E.: Particle fluxes associated with mesoscale eddies in the Sargasso Sea, Deep Sea Res. II, 55, 1426–1444, 2008.

Buesseler, K. O., Pike, S., Maiti, K., Lamborg, C. H., Siegel, D. A., and Trull, T. W.: Thorium-234 as a tracer of spatial, temporal and vertical variability in particle flux in the North Pacific, Deep Sea Res. I, 56, 1143–1167, 2009.

BGD
8, 9535–9576, 2011

Cai, P. H., Dai, M. H., Lv, D. W., and Chen, W. F.: An improvement in the small-volume technique for determining thorium-234 in seawater, Mar. Chem., 100, 282–288, 2006.
Cai, P. H., Chen, W. F., Dai, M. H., Wan, Z. W., Wang, D. X., Li, Q., Tang, T. T., and Lv, D. W.: A high-resolution study of particle export in the southern South China Sea based on ^{234}Th:^{238}U disequilibrium, J. Geophys. Res., Oceans, 113, C04019, doi:10.1029/2007JC004268, 2008.
Chen, W. F.: On the Export Fluxes, Seasonality and Controls of Particulate Organic Carbon in the Northern South China Sea, PhD dissertation, Xiamen Univ. Xiamen, China, 2008 (in Chinese).
Chen, J. H., Edwards, R. L., and Wasserburg, G. J.: ^{238}U, ^{234}U and ^{232}Th in Seawater, Earth. Planet. Sci. Lett., 80, 241–251, 1986.
Chiswell, S. M.: Variability in sea surface temperature around New Zealand from AVHRR images, N. Z. J. Mar. Freshwater Res., 28, 179–192, 1994.
Chiswell, S. M.: Variability in the Southland Current, New Zealand, N. Z. J. Mar. Freshwater Res., 30, 1–17, 1996.
Clementson, L. A., Parslow, J. S., Griffiths, F. B., Lyne, V. D., Mackey, D. J., Harris, G. P., McKenzie, D. C., Bonham, P. I., Rathbone, C. A., and Rintoul, S.: Controls on phytoplankton production in the Australasian sector of the subtropical convergence, Deep Sea Res. I, 45, 1627–1661, 1998.
Coale, K. H. and Bruland, K. W.: ^{234}Th:^{238}U disequilibria within the California Current, Limnol. Oceanogr., 30, 22–33, 1985.
Coale, K. H. and Bruland, K. W.: Oceanic stratified Euphotic Zone as elucidated by ^{234}Th:^{238}U disequilibria, Limnol. Oceanogr., 32, 189–200, 1987.
Cochran, J. K. and Masque, P.: Short-lived U/Th Series radionuclides in the ocean: tracers for scavenging rates, export fluxes and particle dynamics, Rev. Mineral. Geochem., 52, 461–492, 2003.
Comiso, J. C., Mcclain, C. R., Sullivan, C. W., Ryan, J. P., and Leonard, C. L.: Coastal Zone Color Scanner Pigment Concentrations in the Southern-Ocean and Relationships to Geophysical Surface-Features, J. Geophys. Res., Oceans, 98, 2419–2451, 1993.
Coppola, L., Roy-Barman, M., Mulsow, S., Povinec, P., and Jeandel, C.: Low particulate organic carbon export in the frontal zone of the Southern Ocean (Indian sector) revealed by ^{234}Th, Deep Sea Res. I, 52, 51–68, 2005.
Dai, M. H. and Benitez-Nelson, C. R.: Colloidal organic carbon and ^{234}Th in the Gulf of Maine,

BGD
8, 9535–9576, 2011

Mar. Chem., 74, 181–196, 2001.
Froneman, P. W., McQuaid, C. D., and Laubscher, R. K.: Size-fractionated primary production studies in the vicinity of the Subtropical Front and an adjacent warm-core eddy south of Africa in austral winter, J. Plankton Res., 21, 2019–2035, 1999.
Gall, M., Hawes, I., and Boyd, P.: Predicting rates of primary production in the vicinity of the Subtropical Convergence east of New Zealand, N. Z. J. Mar. Freshwater Res., 33, 443–455, 1999.
Hall, J. A., James, M. R., and Bradford-Grieve, J. M.: Structure and dynamics of the pelagic microbial food web of the Subtropical Convergence region east of New Zealand, Aquat. Microb. Ecol., 20, 95–105, 1999.
Heath, R. A.: Oceanic Fronts around Southern New Zealand, Deep Sea Res., 28, 547–560, 1981.
Heath, R. A.: A review of the physical oceanography of the seas around New Zealand-1982, N. Z. J. Mar. Freshwater Res., 19, 79–124, 1985.
Kara, A. B., Rochford, P. A., and Hurlburt, H. E.: An optimal definition for ocean mixed layer depth, J. Geophys. Res., Oceans, 105, 16783–16801, 2000.
Kawakami, H. and Honda, M. C.: Time-series observation of POC fluxes estimated from ^{234}Th in the northwestern North Pacific, Deep Sea Res. I, 1070–1090, 2007.
Knap, A., Michaels, A., Close A., Ducklow, H., and Dickson, A.: Protocols for the Joint Global Ocean Flux Study (JGOFS) core measurements, JGOFS Report Nr. 19: vi-170 pp. (Reprint of the IOC Manuals and Guides No. 29, UNESCO 1994), 1996.
Longhurst, A.: Ecological Geography of the Sea, Academic Press, San Diego, California, 398 pp., 1998.
Michaels, A. F. and Silver, M. W.: Primary production, sinking fluxes and the microbial food web, Deep Sea Res., 35, 473–490, 1988.
Murphy, R. J., Pinkerton, M. H., Richardson, K. M., Bradford-Grieve, J. M., and Boyd, P. W.: Phytoplankton distributions around New Zealand derived from SeaWiFS remotely-sensed ocean colour data, N. Z. J. Mar. Freshwater Res., 35, 343–362, 2001.
Nodder, S. D.: Short-term sediment trap fluxes from Chatham Rise, southwest Pacific Ocean, Limnol. Oceanogr., 42, 777–783, 1997.
Nodder, S. D. and Alexander, B. L.: Sources of variability in geographical and seasonal differences in particulate fluxes from short-term sediment trap deployments, east of New Zealand, Deep Sea Res. II, 45, 1739–1764, 1998.

BGD
8, 9535–9576, 2011

Nodder, S. D. and Gall, M.: Pigment fluxes from the Subtropical Convergence region, east of New Zealand: relationship to planktonic community structure, N. Z. J. Mar. Freshwater Res., 32, 441–465, 1998.

Nodder, S. D. and Northcote, L. C.: Episodic particulate fluxes at southern temperate mid-latitudes (42-45 degrees S) in the Subtropical Front region, east of New Zealand, Deep Sea Res. I, 48, 833–864, 2001.

Nodder, S. D., Pilditch, C. A., Probert, P. K., and Hall, J.: Variability in benthic biomass and activity beneath the Subtropical Front, Chatham Rise, SW Pacific Ocean, Deep Sea Res. I, 50, 959–985, 2003.

Nodder, S. D., Duineveld, G. C. A., Pilditch, C. A., Sutton, P., Probert, P. K., Lavaleye, M. S., Withbaard, R., Chang, F. H., Hall, J., and Richardson, K.: Focusing of phytodetritus deposition beneath a deep-ocean front, Chatham Rise, New Zealand, Limnol. Oceanogr., 52, 299–314, 2007.

Orsi, A. H., Whitworth III, T., and Nowlin, J.: On the meridional extent and fronts of the Circumpolar Current, Deep Sea Res. I, 42, 641–673, 1995.

Pollard, R. T., Salter, I., Sanders, R. J., Lucas, M. I., Moore, C. M., Mills, R. A., Statham, P. J., Allen, J. T., Baker, A. R., Bakker, D. C. E., Charette, M. A., Fielding, S., Fones, G. R., French, M., Hickman, A. E., Holland, R. J., Hughes, J. A., Jickells, T. D., Lampitt, R. S., Morris, P. J., Nedelec, F. H., Nielsdottir, M., Planquette, H., Popova, E. E., Poulton, A. J., Read, J. F., Seeyave, S., Smith, T., Stinchcombe, M., Taylor, S., Thomalla, S., Venables, H. J., Williamson, R., and Zubkov, M. V.: Southern Ocean deep-water carbon export enhanced by natural iron fertilization, Nature, 457, 577–U581, 2009.

Probert, P. K. and McKnight, D. G.: Biomass of bathyal macrobethos in the region of the Subtropical Covergence, Chatham Rise, New Zealand, Deep Sea Res. I, 40, 1003–1007, 1993.

Redfield, A. C., Ketchum, B. H., and Richards, F. A.: The influence of organisms on the composition of sea-water, in: The Sea, Volume 2, M.N. Hill, editor, Interscience Publishers, John Wiley & Sons, 26–27, 1963.

Rutgers van der Loeff, M. M., Friedrich, J., and Bathmann, U. V.: Carbon export during the Spring Bloom at the Antarctic Polar Front, determined with the natural tracer ^{234}Th, Deep Sea Res. II, 44, 457–478, 1997.

Rutgers van der Loeff, M. M., Buesseler, K. O., Bathmann, U. V., Hense, I., and Andrews, J.: Comparison of carbon and opal export rates between summer and spring bloom periods in the region of the Antarctic Polar Front, SE Atlantic., Deep Sea Res. II, 49, 1507–1518, 2002.

BGD

8, 9535–9576, 2011

Savoye, N., Benitez-Nelson, C., Burd, A. B., Cochran, J. K., Charette, M., Buesseler, K. O., Jackson, G. A., Roy-Barman, M., Schmidt, S., and Elskens, M.: ^{234}Th sorption and export models in the water column: A review, Mar. Chem., 100, 234–249, 2006.

Sutton, P.: Detailed structure of the Subtropical Front over Chatham Rise, east of New Zealand, J. Geophys. Res., Oceans, 106, 31045–31056, 2001.

Uddstrom, M. and Oien, N.: On the use of high-resolution satellite data to describe the spatial and temporal variability of sea surface temperatures in the New Zealand region, J. Geophys. Res., 104, 20729–20751, 1999.

Waples, J. T., Benitez-Nelson, C., Savoye, N., Van der Loeff, M. R., Baskaran, M., and Gustafsson, O.: An introduction to the application and future use of ^{234}Th in aquatic systems, Mar. Chem., 100, 166–189, 2006.

Zeldis, J., James, M. R., Grieve, J., and Richards, L.: Omnivory by copepods in the New Zealand Subtropical Frontal Zone, J. Plankton Res., 24, 9–23, 2002.

BGD
8, 9535–9576, 2011

Table 1. Temperature, Salinity, Particulate and Total ^{234}Th activities, ^{238}U activities, ^{234}Th:^{238}U and POC: ^{234}Th ratios for all stations in the Subtropical Front, Chatham Rise, New Zealand, measured in May–June 2008.

Depth m	Temp. °C	Salinity	Particulate ^{234}Th dpm l^{-1}	Total ^{234}Th dpm l^{-1}	^{238}U dpm l^{-1}	POC µmol C l^{-1}	^{234}Th:^{238}U	C:Th ratio µmol C dpm^{-1}
High salinity stations								
C1, 174°36′ E, 42°53′ S, 1010 m								
10	12.979	34.769	0.17 ± 0.01	1.42 ± 0.09	2.46	2.86	0.58 ± 0.04	17.08 ± 1.08
20	12.980	34.769	0.14 ± 0.01	1.69 ± 0.06	2.46	2.90	0.69 ± 0.03	20.37 ± 1.69
50	12.989	34.771	0.15 ± 0.01	1.72 ± 0.06	2.46	2.68	0.70 ± 0.03	17.85 ± 1.22
70	12.992	34.772	0.22 ± 0.01	1.40 ± 0.06	2.46	3.12	0.57 ± 0.02	14.25 ± 0.72
100	13.020	34.786	0.21 ± 0.01	1.50 ± 0.06	2.46	2.39	0.61 ± 0.02	11.61 ± 0.70
C2, 175°56′ E, 42°50′ S, 687 m								
10	15.256	35.247	0.28 ± 0.01	1.64 ± 0.09	2.50	3.28	0.66 ± 0.03	11.65 ± 0.53
20	15.234	35.242	0.29 ± 0.01	1.85 ± 0.06	2.50	3.84	0.74 ± 0.03	13.38 ± 0.63
50	15.207	35.235	0.26 ± 0.01	1.65 ± 0.07	2.49	3.65	0.66 ± 0.03	14.31 ± 0.68
70	15.168	35.226	0.28 ± 0.01	2.05 ± 0.09	2.49	3.40	0.82 ± 0.03	12.17 ± 0.54
100	14.564	35.129	0.30 ± 0.01	1.89 ± 0.07	2.49	2.35	0.76 ± 0.03	7.73 ± 0.35
C3, 175°13′ E, 43°11′ S, 125 m								
10	12.983	34.885	0.15 ± 0.01	1.63 ± 0.08	2.47	2.77	0.66 ± 0.03	18.68 ± 1.41
20	12.990	34.884	0.16 ± 0.01	1.93 ± 0.07	2.47	2.80	0.78 ± 0.03	18.07 ± 1.42
50	13.002	34.886	0.15 ± 0.01	1.45 ± 0.06	2.47	2.82	0.59 ± 0.03	19.10 ± 1.40
70	12.998	34.884	0.14 ± 0.01	1.75 ± 0.06	2.47	2.51	0.71 ± 0.02	17.54 ± 1.24
100	12.917	34.868	0.15 ± 0.01	1.85 ± 0.06	2.47	1.98	0.75 ± 0.03	13.64 ± 1.12
C3 repeat (after 16 days)								
10	12.487	34.867	0.25 ± 0.04	1.62 ± 0.11	2.47	2.37	0.66 ± 0.04	9.40 ± 1.38
20	12.490	34.867	0.20 ± 0.04	1.52 ± 0.14	2.47	1.98	0.61 ± 0.06	10.16 ± 2.12
50	12.490	34.867	0.26 ± 0.04	1.50 ± 0.11	2.47	2.06	0.61 ± 0.04	8.08 ± 1.14
70	12.498	34.868	0.26 ± 0.04	1.61 ± 0.10	2.47	2.27	0.65 ± 0.04	8.60 ± 1.17
100	12.404	34.856	0.34 ± 0.04	1.57 ± 0.11	2.47	2.13	0.64 ± 0.04	6.34 ± 0.77
C4, 176°03′ E, 43°29′ S, 387 m								
10	13.030	34.911	0.20 ± 0.01	1.74 ± 0.08	2.47	3.65	0.71 ± 0.03	18.15 ± 1.06
20	13.030	34.911	0.18 ± 0.01	1.83 ± 0.07	2.47	2.88	0.74 ± 0.03	15.80 ± 1.08
50	13.043	34.913	0.21 ± 0.01	1.89 ± 0.07	2.47	3.61	0.76 ± 0.03	17.05 ± 0.96
70	13.047	34.913	0.10 ± 0.01	1.81 ± 0.06	2.47	2.88	0.74 ± 0.02	28.72 ± 2.65
100	12.404	34.837	0.24 ± 0.01	1.98 ± 0.08	2.47	1.08	0.80 ± 0.03	4.42 ± 0.24

BGD
8, 9535–9576, 2011

Table 1. Continued.

Depth m	Temp. °C	Salinity	Particulate ^{234}Th dpm l^{-1}	Total ^{234}Th dpm l^{-1}	^{238}U dpm l^{-1}	POC µmol C l^{-1}	^{234}Th:^{238}U	C:Th ratio µmol C dpm^{-1}
C7, 178°22′ E, 42°45′ S, 1124 m								
10	14.619	35.209	0.23 ± 0.01	1.88 ± 0.07	2.49	3.31	0.76 ± 0.03	14.46 ± 0.78
25	14.611	35.208	0.21 ± 0.01	1.88 ± 0.07	2.49	2.89	0.75 ± 0.03	13.62 ± 0.83
35	14.570	35.197	0.21 ± 0.01	1.83 ± 0.07	2.49	3.06	0.71 ± 0.03	14.32 ± 0.78
50	14.034	35.083	0.20 ± 0.01	1.75 ± 0.06	2.48	2.88	0.70 ± 0.03	14.13 ± 0.78
75	13.549	34.971	0.17 ± 0.01	1.85 ± 0.07	2.48	3.38	0.75 ± 0.03	20.27 ± 1.50
120	13.139	35.052	0.33 ± 0.01	2.11 ± 0.06	2.48	1.89	0.85 ± 0.03	5.73 ± 0.24
250	10.089	34.705	0.24 ± 0.02	2.09 ± 0.08	2.46	1.58	0.85 ± 0.03	6.55 ± 0.44
500	8.409	34.563	0.29 ± 0.01	1.97 ± 0.07	2.45	2.13	0.81 ± 0.03	7.41 ± 0.34
750	6.764	34.457	0.16 ± 0.01	2.41 ± 0.08	2.44	0.76	0.99 ± 0.03	4.74 ± 0.33
1090	5.123	34.436	0.22 ± 0.01	2.16 ± 0.07	2.44	1.56	0.89 ± 0.03	7.06 ± 0.41
C8, 178°49′ E, 42°49′ S, 1096 m								
10	14.266	35.115	0.23 ± 0.01	1.81 ± 0.07	2.49	2.33	0.73 ± 0.03	10.34 ± 0.56
25	14.231	35.115	0.21 ± 0.01	1.86 ± 0.04	2.49	2.36	0.75 ± 0.02	11.38 ± 0.71
50	14.220	35.113	0.25 ± 0.01	2.02 ± 0.08	2.49	2.24	0.81 ± 0.03	9.11 ± 0.46
75	14.214	35.104	0.24 ± 0.01	1.82 ± 0.07	2.49	2.25	0.73 ± 0.03	9.42 ± 0.47
120	12.534	34.848	0.26 ± 0.01	2.02 ± 0.08	2.47	1.24	0.82 ± 0.03	4.69 ± 0.25
C9, 174°36′ E, 42°53′ S, 1010 m								
10	14.069	35.113	0.24 ± 0.01	1.99 ± 0.07	2.49	2.10	0.80 ± 0.03	8.82 ± 0.46
20	14.031	35.104	0.26 ± 0.01	2.19 ± 0.08	2.49	2.47	0.88 ± 0.03	9.51 ± 0.50
45	14.049	35.107	0.26 ± 0.01	2.11 ± 0.07	2.49	1.55	0.85 ± 0.03	5.92 ± 0.30
70	13.885	35.066	0.27 ± 0.01	1.97 ± 0.08	2.48	1.73	0.79 ± 0.03	6.36 ± 0.28
100	13.736	35.033	0.19 ± 0.01	2.05 ± 0.07	2.48	2.13	0.83 ± 0.03	11.48 ± 0.76
C10, 178°17′ E, 42°50′ S, 662 m								
10	14.443	35.246	0.16 ± 0.01	2.17 ± 0.08	2.50	1.96	0.87 ± 0.03	11.88 ± 0.78
20	14.432	35.245	0.19 ± 0.01	2.06 ± 0.07	2.50	1.99	0.83 ± 0.03	10.32 ± 0.65
45	14.434	35.242	0.18 ± 0.01	2.08 ± 0.08	2.50	1.94	0.83 ± 0.03	10.52 ± 0.64
70	14.433	35.242	0.19 ± 0.01	2.11 ± 0.07	2.50	2.53	0.85 ± 0.03	13.03 ± 0.72
100	14.399	35.233	0.23 ± 0.01	2.21 ± 0.07	2.49	1.34	0.88 ± 0.03	5.90 ± 0.33
C11, 178°42′ E, 42°58′ S, 528 m								
10	13.748	35.041	0.15 ± 0.01	1.98 ± 0.06	2.48	3.28	0.80 ± 0.03	21.26 ± 1.43
20	13.724	35.035	0.15 ± 0.01	1.87 ± 0.06	2.48	2.91	0.75 ± 0.02	19.69 ± 1.52
45	13.684	35.025	0.15 ± 0.01	1.97 ± 0.05	2.48	2.30	0.80 ± 0.02	15.73 ± 1.09
70	13.646	35.026	0.15 ± 0.01	1.93 ± 0.04	2.48	1.97	0.78 ± 0.02	13.40 ± 0.91
100	13.411	34.994	0.15 ± 0.01	2.47 ± 0.08	2.48	1.86	1.00 ± 0.03	12.11 ± 0.92

BGD
8, 9535–9576, 2011

Table 1. Continued.

Depth m	Temp. °C	Salinity	Particulate ^{234}Th dpm l^{-1}	Total ^{234}Th dpm l^{-1}	^{238}U dpm l^{-1}	POC µmol C l^{-1}	^{234}Th:^{238}U	C:Th ratio µmol C dpm^{-1}
C12, 177°30′ E, 43°42′ S, 342 m								
10	13.362	35.053	0.11 ± 0.01	1.87 ± 0.06	2.48	1.56	0.75 ± 0.02	14.49 ± 1.31
20	13.366	35.053	0.15 ± 0.01	1.95 ± 0.06	2.48	1.54	0.79 ± 0.02	10.24 ± 0.75
45	13.365	35.053	0.13 ± 0.01	2.00 ± 0.06	2.48	1.59	0.80 ± 0.03	12.00 ± 0.90
70	13.366	35.053	0.13 ± 0.01	1.84 ± 0.06	2.48	1.60	0.74 ± 0.02	12.70 ± 0.99
100	13.079	35.000	0.18 ± 0.01	1.89 ± 0.08	2.48	1.24	0.76 ± 0.03	6.92 ± 0.46
C13, 178°31′ E, 43°42′ S, 422 m								
10	13.603	35.025	0.12 ± 0.01	2.03 ± 0.07	2.48	1.86	0.82 ± 0.03	15.22 ± 1.26
20	13.602	35.025	0.11 ± 0.01	2.11 ± 0.07	2.48	2.10	0.85 ± 0.03	19.76 ± 2.09
45	13.608	35.024	0.13 ± 0.01	2.05 ± 0.07	2.48	2.57	0.83 ± 0.03	20.34 ± 1.57
70	13.658	35.045	0.12 ± 0.01	1.91 ± 0.07	2.48	1.97	0.78 ± 0.03	15.86 ± 1.21
100	11.842	34.842	0.21 ± 0.01	2.32 ± 0.07	2.47	0.98	0.94 ± 0.03	4.65 ± 0.28
C21, 175°20′ E, 43°68′ S, 356 m								
10	12.437	34.854	0.19 ± 0.03	1.70 ± 0.11	2.47	2.36	0.69 ± 0.04	12.68 ± 2.19
20	12.442	34.854	0.27 ± 0.04	1.86 ± 0.13	2.47	2.74	0.75 ± 0.05	10.22 ± 1.42
50	12.437	34.853	0.15 ± 0.03	2.14 ± 0.11	2.47	2.54	0.87 ± 0.05	16.97 ± 3.50
70	12.438	34.853	0.26 ± 0.03	2.00 ± 0.11	2.47	2.30	0.81 ± 0.05	8.91 ± 1.05
100	12.419	34.850	0.27 ± 0.04	2.20 ± 0.12	2.47	2.36	0.89 ± 0.05	8.68 ± 1.19
Mid-salinity stations								
C5, 176°30′ E, 43°39′ S, 367 m								
10	11.433	34.481	0.46 ± 0.02	1.96 ± 0.08	2.44	5.19	0.80 ± 0.03	11.35 ± 0.39
20	11.433	34.480	0.56 ± 0.02	1.85 ± 0.07	2.44	5.59	0.76 ± 0.03	9.98 ± 0.30
50	11.647	34.536	0.40 ± 0.01	2.00 ± 0.07	2.45	4.14	0.82 ± 0.03	10.44 ± 0.38
70	11.547	34.616	0.33 ± 0.01	2.11 ± 0.08	2.45	3.57	0.86 ± 0.03	10.88 ± 0.45
100	10.886	34.701	0.18 ± 0.01	2.09 ± 0.08	2.46	1.17	0.85 ± 0.03	6.55 ± 0.47
150	10.467	34.727	0.23 ± 0.01	2.13 ± 0.07	2.46	1.34	0.87 ± 0.03	5.95 ± 0.33
250	9.539	34.664	0.24 ± 0.01	2.00 ± 0.07	2.45	0.96	0.82 ± 0.03	4.07 ± 0.21
340	8.930	34.606	0.35 ± 0.01	1.84 ± 0.08	2.45	1.90	0.75 ± 0.03	5.47 ± 0.21
C6, 178°22′ E, 43°02′ S, 340 m								
10	11.660	34.536	0.53 ± 0.02	1.60 ± 0.05	2.45	6.07	0.65 ± 0.02	11.57 ± 0.36
20	11.664	34.536	0.55 ± 0.02	1.76 ± 0.07	2.45	5.68	0.72 ± 0.03	10.42 ± 0.33
50	11.672	34.538	0.57 ± 0.02	1.82 ± 0.06	2.45	6.09	0.74 ± 0.03	10.64 ± 0.31
70	11.679	34.544	0.54 ± 0.02	1.80 ± 0.07	2.45	5.38	0.73 ± 0.03	9.89 ± 0.29
100	11.247	34.740	0.20 ± 0.01	1.96 ± 0.06	2.46	1.77	0.80 ± 0.03	8.96 ± 0.58

BGD
8, 9535–9576, 2011

Table 1. Continued.

Depth m	Temp. °C	Salinity	Particulate ^{234}Th dpm l^{-1}	Total ^{234}Th dpm l^{-1}	^{238}U dpm l^{-1}	POC µmol C l^{-1}	^{234}Th:^{238}U	C:Th ratio µmol C dpm^{-1}
150	10.601	34.728	0.19 ± 0.01	2.10 ± 0.15	2.46	1.10	0.86 ± 0.03	5.90 ± 0.38
250	8.966	34.605	0.11 ± 0.01	2.11 ± 0.08	2.45	0.40	0.86 ± 0.03	3.73 ± 0.36
315	8.452	34.546	0.33 ± 0.01	1.45 ± 0.06	2.45	1.55	0.60 ± 0.02	4.76 ± 0.21
C14, 178°20′ E, 44°14′ S, 526 m								
10	10.837	34.340	0.67 ± 0.02	1.75 ± 0.07	2.43	3.59	0.72 ± 0.03	5.39 ± 0.14
20	10.858	34.344	0.67 ± 0.02	1.91 ± 0.06	2.43	1.96	0.79 ± 0.02	2.93 ± 0.08
45	11.021	34.390	0.69 ± 0.02	2.00 ± 0.06	2.44	3.69	0.82 ± 0.03	5.37 ± 0.14
70	11.099	34.438	0.64 ± 0.02	1.93 ± 0.07	2.44	3.25	0.79 ± 0.03	5.10 ± 0.13
100	10.485	34.578	0.21 ± 0.01	2.21 ± 0.07	2.45	1.09	0.90 ± 0.03	5.26 ± 0.31
150	10.485	34.590	n.d.	2.41 ± 0.08	2.45	0.79	0.98 ± 0.03	
C15, 177°48′ E, 44°24′ S, 716 m								
10	11.109	34.386	0.69 ± 0.02	1.94 ± 0.07	2.43	4.65	0.80 ± 0.03	6.76 ± 0.18
20	11.096	34.383	0.70 ± 0.02	1.68 ± 0.06	2.43	4.38	0.69 ± 0.03	6.29 ± 0.17
50	10.905	34.353	0.43 ± 0.02	1.98 ± 0.07	2.43	2.33	0.81 ± 0.03	5.36 ± 0.19
70	11.029	34.416	0.41 ± 0.01	2.27 ± 0.09	2.44	1.74	0.93 ± 0.04	4.26 ± 0.15
100	10.879	34.626	0.17 ± 0.01	2.35 ± 0.08	2.45	0.88	0.96 ± 0.03	5.13 ± 0.38
C16, 178°28′ E, 44°33′ S, 1078 m								
10	10.361	34.265	0.66 ± 0.02	1.76 ± 0.07	2.43	4.06	0.72 ± 0.03	6.18 ± 0.17
20	10.380	34.270	0.65 ± 0.02	1.75 ± 0.07	2.43	3.57	0.72 ± 0.03	5.52 ± 0.16
40	10.409	34.277	0.55 ± 0.02	1.84 ± 0.06	2.43	3.66	0.76 ± 0.03	6.71 ± 0.20
65	10.824	34.465	0.46 ± 0.02	1.72 ± 0.06	2.44	2.32	0.71 ± 0.03	5.00 ± 0.16
100	9.767	34.531	0.23 ± 0.02	2.39 ± 0.08	2.45	1.26	0.98 ± 0.03	5.56 ± 0.33
C20, 178°22′ E, 43°37′ S, 364 m								
10	11.234	34.579	0.36 ± 0.04	2.12 ± 0.13	2.45	4.10	0.86 ± 0.05	11.51 ± 1.18
20	11.235	34.579	0.31 ± 0.04	1.87 ± 0.12	2.45	4.65	0.76 ± 0.05	14.87 ± 2.02
50	11.224	34.579	0.50 ± 0.04	2.17 ± 0.13	2.45	4.15	0.89 ± 0.06	8.29 ± 0.63
70	11.223	34.579	0.39 ± 0.03	2.01 ± 0.17	2.45	3.95	0.82 ± 0.07	10.11 ± 0.91
120	11.137	34.641	0.35 ± 0.04	2.12 ± 0.13	2.45	2.86	0.86 ± 0.05	8.26 ± 0.97
250	9.409	34.608	0.36 ± 0.04	2.54 ± 0.14	2.45	0.92	1.04 ± 0.06	2.53 ± 0.25
350	8.890	34.585	0.35 ± 0.04	1.87 ± 0.14	2.45	1.33	0.76 ± 0.06	3.80 ± 0.43
C22, 175°20′ E, 43°99′ S, 470 m								
10	10.870	34.593	0.33 ± 0.03	2.07 ± 0.12	2.45	4.13	0.85 ± 0.05	12.53 ± 1.31
20	10.880	34.595	0.29 ± 0.04	2.18 ± 0.14	2.45	4.03	0.89 ± 0.06	13.66 ± 1.79
50	10.811	34.581	0.41 ± 0.04	2.18 ± 0.13	2.45	4.61	0.89 ± 0.05	11.22 ± 0.99
70	10.732	34.567	0.37 ± 0.03	2.06 ± 0.12	2.45	3.31	0.84 ± 0.05	8.88 ± 0.78
100	10.689	34.565	0.33 ± 0.04	1.96 ± 0.12	2.45	3.15	0.80 ± 0.05	9.46 ± 1.18

BGD
8, 9535–9576, 2011

Table 1. Continued.

Depth m	Temp. °C	Salinity	Particulate ^{234}Th dpm l^{-1}	Total ^{234}Th dpm l^{-1}	^{238}U dpm l^{-1}	POC µmol C l^{-1}	^{234}Th:^{238}U	C:Th ratio µmol C dpm^{-1}
D1, 174°65′ E, 43°65′ S, 510 m								
10	9.928	34.443	0.30 ± 0.03	1.95 ± 0.12	2.44	4.17	0.80 ± 0.05	14.06 ± 1.64
20	9.980	34.451	0.27 ± 0.04	1.91 ± 0.14	2.44	4.31	0.78 ± 0.06	15.78 ± 2.39
50	10.005	34.455	0.29 ± 0.04	1.72 ± 0.12	2.44	4.03	0.71 ± 0.05	14.09 ± 1.73
70	9.966	34.448	0.29 ± 0.03	2.00 ± 0.13	2.44	4.14	0.82 ± 0.05	14.34 ± 1.66
100	9.945	34.452	0.27 ± 0.04	2.22 ± 0.13	2.44	2.28	0.91 ± 0.05	8.35 ± 1.18
C4 repeat (after 11.6 days)								
10	10.975	34.542	0.47 ± 0.04	2.19 ± 0.13	2.45	5.61	0.90 ± 0.05	11.82 ± 1.09
20	10.975	34.542	0.44 ± 0.05	2.33 ± 0.15	2.45	5.32	0.95 ± 0.06	12.07 ± 1.29
50	10.979	34.542	0.48 ± 0.04	1.44 ± 0.18	2.45	5.19	0.59 ± 0.07	10.71 ± 0.87
70	10.981	34.542	0.43 ± 0.04	1.86 ± 0.13	2.45	5.24	0.76 ± 0.05	12.15 ± 1.10
100	10.980	34.543	0.51 ± 0.05	2.07 ± 0.15	2.45	5.58	0.85 ± 0.06	10.97 ± 1.02
Low salinity stations								
C17, 178°35′ E, 44°21′ S, 1186 m								
10	9.699	34.206	0.45 ± 0.02	1.61 ± 0.06	2.42	3.12	0.66 ± 0.03	6.70 ± 0.23
20	9.698	34.206	0.60 ± 0.05	1.80 ± 0.07	2.42	2.43	0.74 ± 0.03	4.26 ± 0.34
45	9.704	34.206	0.45 ± 0.02	1.65 ± 0.06	2.42	2.34	0.68 ± 0.03	5.21 ± 0.18
65	9.686	34.209	0.25 ± 0.01	1.93 ± 0.07	2.42	1.45	0.79 ± 0.03	5.88 ± 0.29
100	9.363	34.383	0.21 ± 0.01	2.30 ± 0.08	2.43	1.36	0.94 ± 0.03	6.51 ± 0.41
250	7.635	34.422	0.18 ± 0.01	2.34 ± 0.08	2.44	1.01	0.96 ± 0.03	5.51 ± 0.36
500	6.843	34.370	0.22 ± 0.01	2.16 ± 0.07	2.43	1.22	0.90 ± 0.03	5.44 ± 0.30
750	5.563	34.291	0.24 ± 0.01	2.18 ± 0.07	2.43	0.61	0.90 ± 0.03	2.46 ± 0.13
1170	3.253	34.380	0.36 ± 0.02	1.88 ± 0.07	2.43	1.03	0.78 ± 0.03	2.88 ± 0.12
C18, 177°43′ E, 44°06′ S, 942 m								
10	9.699	34.237	0.43 ± 0.02	1.86 ± 0.06	2.42	4.00	0.77 ± 0.03	9.28 ± 0.33
20	9.705	34.239	0.44 ± 0.02	1.85 ± 0.07	2.42	3.92	0.76 ± 0.03	8.92 ± 0.33
45	9.715	34.241	0.46 ± 0.02	1.83 ± 0.06	2.42	3.83	0.76 ± 0.03	8.27 ± 0.28
65	9.974	34.349	0.29 ± 0.01	2.15 ± 0.07	2.43	2.76	0.88 ± 0.03	9.44 ± 0.43
100	9.768	34.464	0.17 ± 0.01	2.10 ± 0.07	2.44	1.07	0.86 ± 0.03	6.39 ± 0.49
250	8.046	34.463	0.23 ± 0.01	2.29 ± 0.08	2.44	0.90	0.94 ± 0.03	4.00 ± 0.23
500	7.013	34.384	0.16 ± 0.01	2.35 ± 0.08	2.43	1.08	0.96 ± 0.03	6.84 ± 0.50
750	5.990	34.312	0.24 ± 0.01	2.21 ± 0.07	2.43	0.74	0.91 ± 0.03	3.03 ± 0.15
890	5.553	34.290	0.28 ± 0.02	2.12 ± 0.07	2.43	1.41	0.87 ± 0.03	5.06 ± 0.44

BGD
8, 9535–9576, 2011

Table 1. Continued.

Depth m	Temp. °C	Salinity	Particulate ^{234}Th dpm l^{-1}	Total ^{234}Th dpm l^{-1}	^{238}U dpm l^{-1}	POC µmol C l^{-1}	^{234}Th:^{238}U	C:Th ratio µmol C dpm^{-1}
C23, 175°17′ E, 44°23′ S, 653 m								
10	9.443	34.252	0.44 ± 0.04	2.08 ± 0.13	2.43	3.68	0.86 ± 0.05	8.40 ± 0.78
20	9.436	34.250	0.32 ± 0.04	1.97 ± 0.17	2.43	3.48	0.81 ± 0.07	11.04 ± 1.55
40	9.441	34.251	0.42 ± 0.04	1.95 ± 0.14	2.43	3.37	0.80 ± 0.06	8.00 ± 0.72
60	9.497	34.270	0.32 ± 0.04	2.03 ± 0.14	2.43	2.99	0.84 ± 0.06	9.26 ± 1.03
80	9.646	34.371	0.45 ± 0.04	1.90 ± 0.13	2.43	2.98	0.78 ± 0.05	6.62 ± 0.64

BGD
8, 9535–9576, 2011

Table 2. Inventories of particulate organic carbon (POC), particulate ^{234}Th and fluorescence, Steady-State (SS) ^{234}Th flux, POC/^{234}Th ratios and POC flux in the upper 100 m and euphotic zone (Ez) within the Subtropical Front in May–June 2008.

Station	Euphotic zone[a] (Ez) m	POC @ 100 m $\times 10^2$ mol C m^{-2}	Part. ^{234}Th @ 100 m $\times 10^4$ dpm m^{-2}	Fluorescence @ 100 m Signal m^{-2}	Fluorescence @ Ez Signal m^{-2}	SS ^{234}Th flux @ 100 m dpm m^{-2} d^{-1}	SS ^{234}Th flux @ Ez[b] dpm m^{-2} d^{-1}	C/Th ratio[c] µmol C dpm^{-1}	POC Flux @ 100 m mmol C m^{-2} d^{-1}
High salinity stations									
C1	160	2.82	1.75 ± 0.041	67.1	85.5	2564 ± 133	3393 ± 168	11.6 ± 0.7	29.8 ± 2.4
C2	170	3.4	2.79 ± 0.047	76.6	93.3	1901 ± 156	2522 ± 205	7.7 ± 0.4	14.7 ± 1.4
C3	100	2.61	1.48 ± 0.040	58.5	58.5	2148 ± 135	2148 ± 135	13.6 ± 1.1	29.3 ± 3.0
C3 repeat	100	2.13	2.54 ± 0.14	39.7	39.7	2627 ± 239	2627 ± 239	6.3 ± 0.8	16.6 ± 2.5
C4	110	2.87	1.80 ± 0.042	98.9	99.9	1768 ± 141	1837 ± 143	4.4 ± 0.2	7.8 ± 0.8
C7	130	3.49	2.66 ± 0.054	75.1	81.0	2059 ± 173	2059 ± 173	5.7 ± 0.2	11.8 ± 1.1
C8	130	2.51	2.84 ± 0.057	34.5	73.6	2003 ± 177	2067 ± 179	4.7 ± 0.2	9.4 ± 1.0
C9	160	1.95	2.50 ± 0.045	54.2	79.3	1195 ± 155	1575 ± 197	11.5 ± 0.8	13.7 ± 2.0
C10	150	2.02	1.93 ± 0.041	62.6	84.9	1104 ± 150	1330 ± 180	5.9 ± 0.3	6.5 ± 1.0
C11	140	2.38	1.49 ± 0.038	39.2	44.5	1343 ± 116	1343 ± 116	12.1 ± 0.9	16.3 ± 1.9
C12	150	1.53	1.39 ± 0.038	39.0	87.8	1631 ± 132	2059 ± 173	6.9 ± 0.5	11.3 ± 1.2
C13	100	1.99	1.33 ± 0.038	54.2	54.2	1198 ± 142	1198 ± 142	4.6 ± 0.3	5.6 ± 0.7
C21	200	2.49	2.28 ± 0.12	50.7	94.9	1349 ± 263	1736 ± 418	8.7 ± 1.2	11.7 ± 2.6
Mid-salinity stations									
C5	100	4.02	3.94 ± 0.054	129.6	129.6	1284 ± 154	1284 ± 154	6.6 ± 0.5	8.4 ± 1.2
C6	100	5.16	4.98 ± 0.058	144.6	144.6	1862 ± 136	1862 ± 136	9.0 ± 0.6	16.7 ± 1.6
C14	100	2.78	5.96 ± 0.059	90.7	90.7	1339 ± 132	1339 ± 132	5.3 ± 0.3	7.0 ± 0.8
C15	100	2.71	4.79 ± 0.058	92.0	92.0	1167 ± 155	1167 ± 155	5.1 ± 0.4	6.0 ± 1.0
C16	100	2.86	4.97 ± 0.058	93.5	93.5	1604 ± 144	1604 ± 144	5.6 ± 0.3	8.9 ± 1.0
C20	160	4.71	4.62 ± 0.18	136.9	149.2	1383 ± 383	1428 ± 385	8.3 ± 1.0	11.4 ± 3.4
C22	150	3.87	3.52 ± 0.13	135.7	158.1	991 ± 263	1395 ± 331	9.5 ± 1.2	9.4 ± 2.8
D1	140	3.88	2.83 ± 0.13	98.9	114.5	1452 ± 263	1562 ± 300	8.4 ± 1.2	12.1 ± 2.8
C4 repeat	150	5.33	4.63 ± 0.16	200.2	243.4	1464 ± 312	1715 ± 376	11.0 ± 1.0	16.1 ± 3.7
Low salinity stations									
C17	120	2.02	3.80 ± 0.085	57.0	58.8	1592 ± 142	1621 ± 149	6.5 ± 0.4	10.4 ± 1.1
C18	130	3.09	3.56 ± 0.053	60.8	63.0	1304 ± 143	1392 ± 148	6.4 ± 0.5	8.3 ± 1.1
C23	150	2.63	3.01 ± 0.11	54.3	61.4	1015 ± 237	1521 ± 237	6.6 ± 0.6	6.7 ± 1.7

[a] The depth of euphotic zone (Ez) is estimated where fluorescence reaches its minimum.

[b] For those stations where Ez>100 m, ^{234}Th was assumed to be in equilibrium with dissolved ^{238}U, and ^{234}Th flux was calculated according to this assumption.

[c] Bottle C/Th ratios @ 100 m are used here, and the calculated POC fluxes should be considered as upper limits on Chatham Rise.

BGD
8, 9535–9576, 2011

Table 3. P values derived from t-tests with unequal variance on inventories of POC, Particulate ^{234}Th and fluorescence, Steady-State (SS) ^{234}Th fluxes and POC fluxes at 100 m and euphotic zone (Ez) water depths for mid- vs. high salinity water and mid- vs. low salinity water.

Item	P value (mid vs. high)	P value (mid vs. low)
POC inventory @ 100 m	0.00206	0.02
Particulate Th @ 100 m	0.0000141	0.03
Flu inventory @ 100 m	0.00031	0.00053
Flu inventory @ Ez	0.0054	0.0018
SS ^{234}Th flux @ 100 m	0.0973	0.66
SS ^{234}Th flux @ Ez	0.0508	0.79
POC flux @ 100 m	0.0998	0.22

BGD
8, 9535–9576, 2011

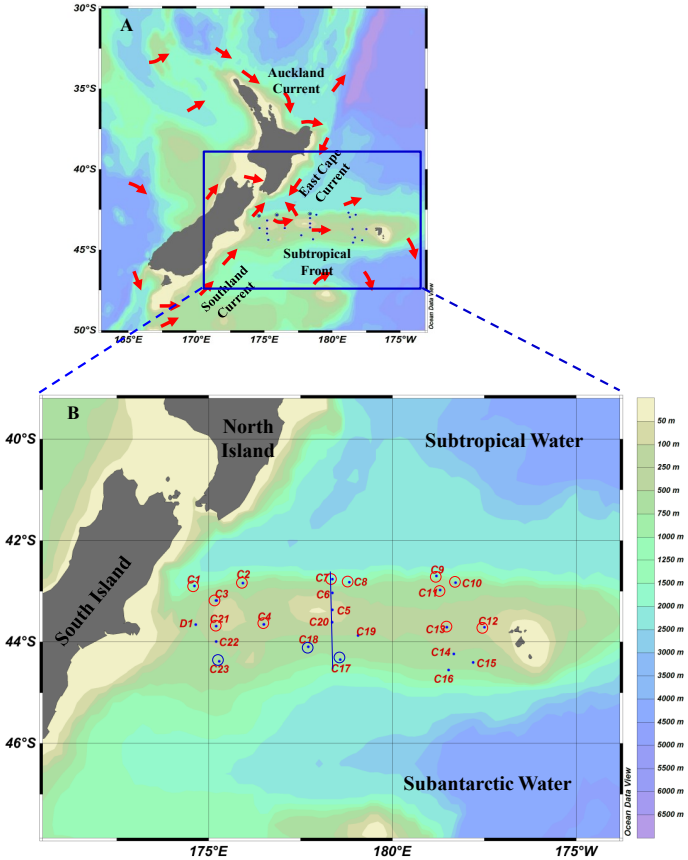

Fig. 1. Map of the study area showing the mean circulation and water masses **(a)** and location of sampling sites during the May–June 2008 research cruise TAN0806 **(b)**. Stations with salinity >34.8 and <34.5 are marked as red and blue circles, respectively. The blue line is the transect that was sampled throughout the whole water column (referred to as Transect *M*). The bathymetry of the study area is also outlined to emphasize the location of Chatham Rise.

BGD
8, 9535–9576, 2011

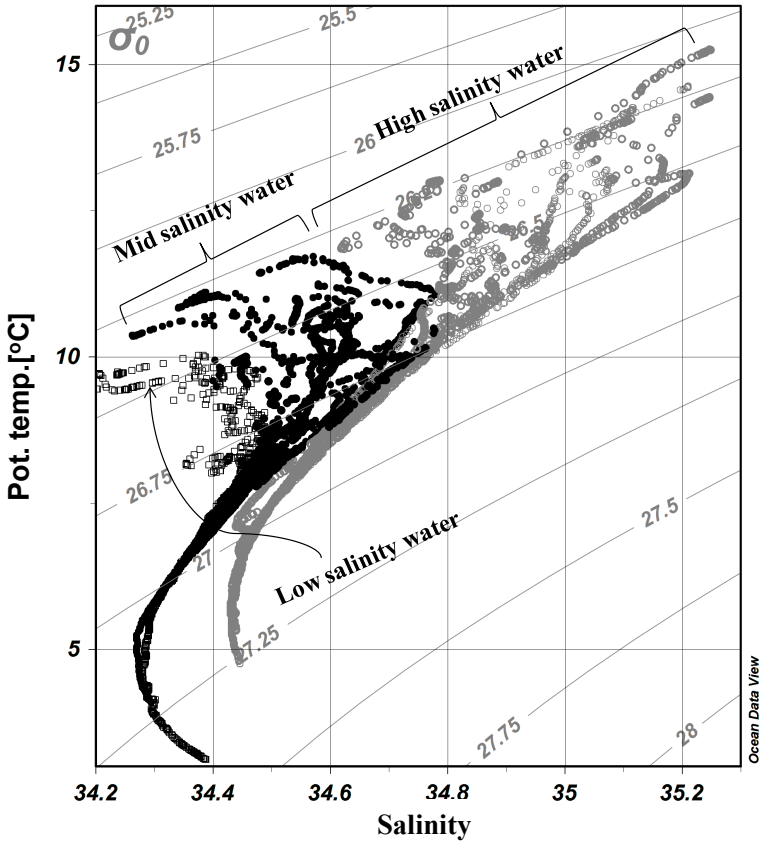

Fig. 2. T-S diagram over Chatham Rise, offshore New Zealand (∘ high salinity ($S > 34.8$) water; • mid-salinity ($34.5 < S < 34.8$) water; □ low salinity ($S < 34.5$) water). The isopycnal lines are also shown.

BGD
8, 9535–9576, 2011

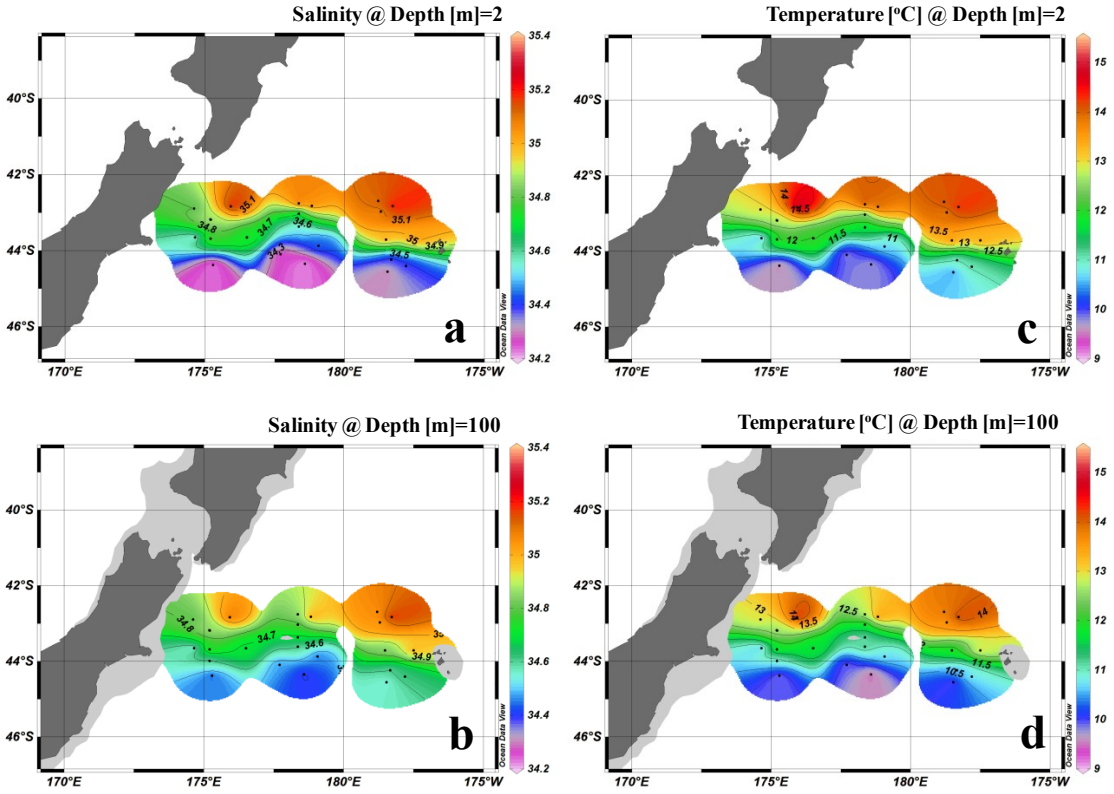

Fig. 3. Distributions of temperature and salinity, highlighting dramatic changes within the Subtropical Frontal zone: **(a)** surface salinity at 2 m water depth, **(b)** salinity at 100 m, **(c)** surface temperature, and **(d)** temperature at 100 m.

BGD
8, 9535–9576, 2011

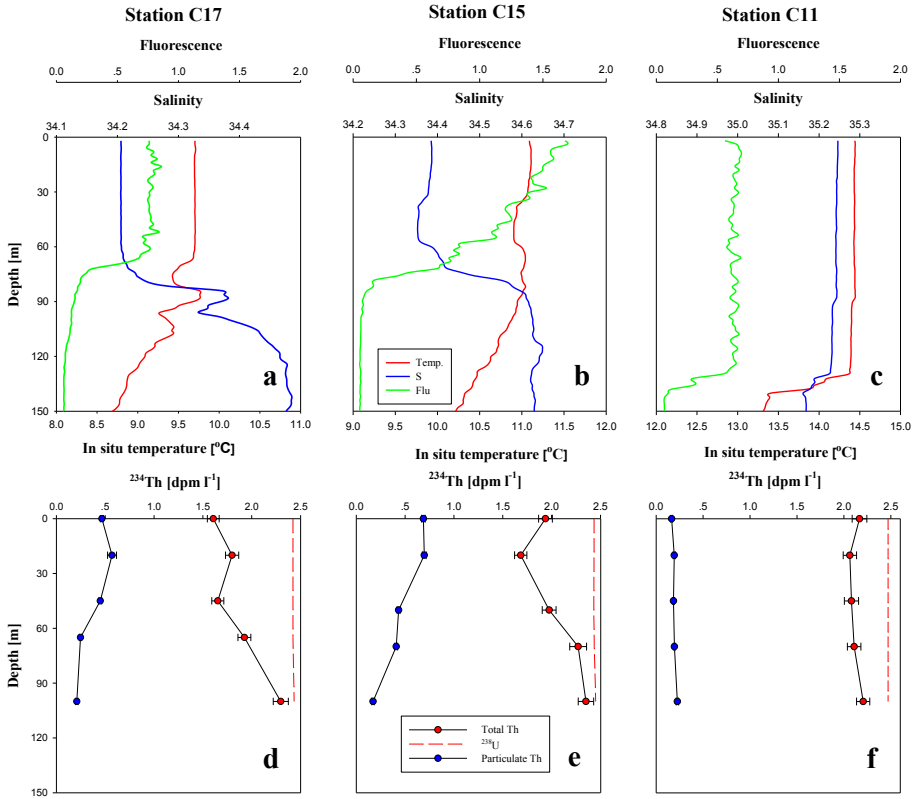

Fig. 4. **(a)**, **(b)**, and **(c)** are vertical profiles of temperature, salinity and fluorescence in the upper 100 m at stations C17, C15, and C11, respectively. **(d)**, **(e)**, and **(f)** are vertical profiles of particulate and total ^{234}Th from the same stations.

BGD
8, 9535–9576, 2011

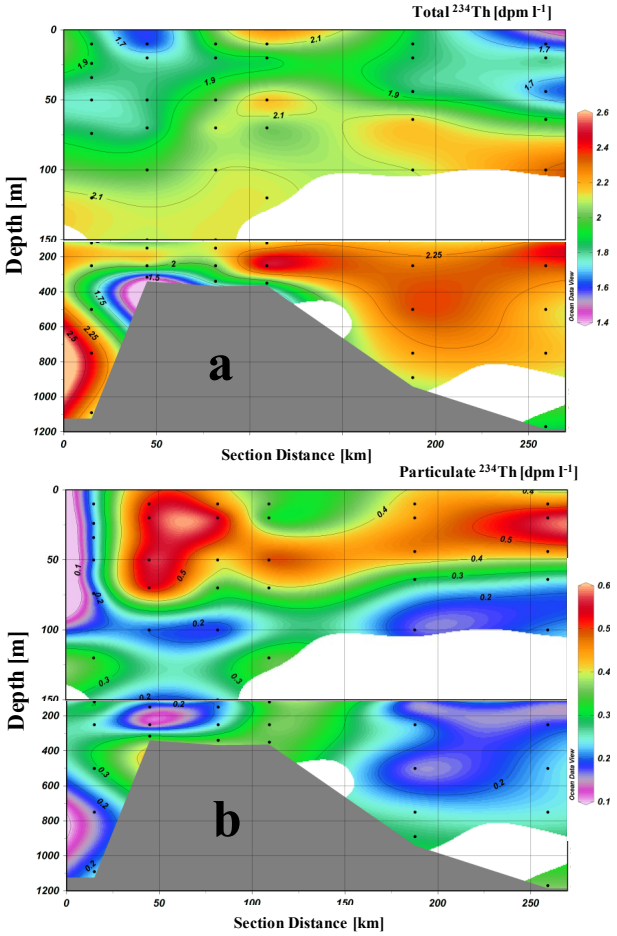

Fig. 5. Sectional distributions of ^{234}Th activity along a meridional transect (Transect *M*) across the Chatham Rise (see Fig. 1 for transect location): **(a)** total ^{234}Th and **(b)** particulate ^{234}Th.

BGD
8, 9535–9576, 2011

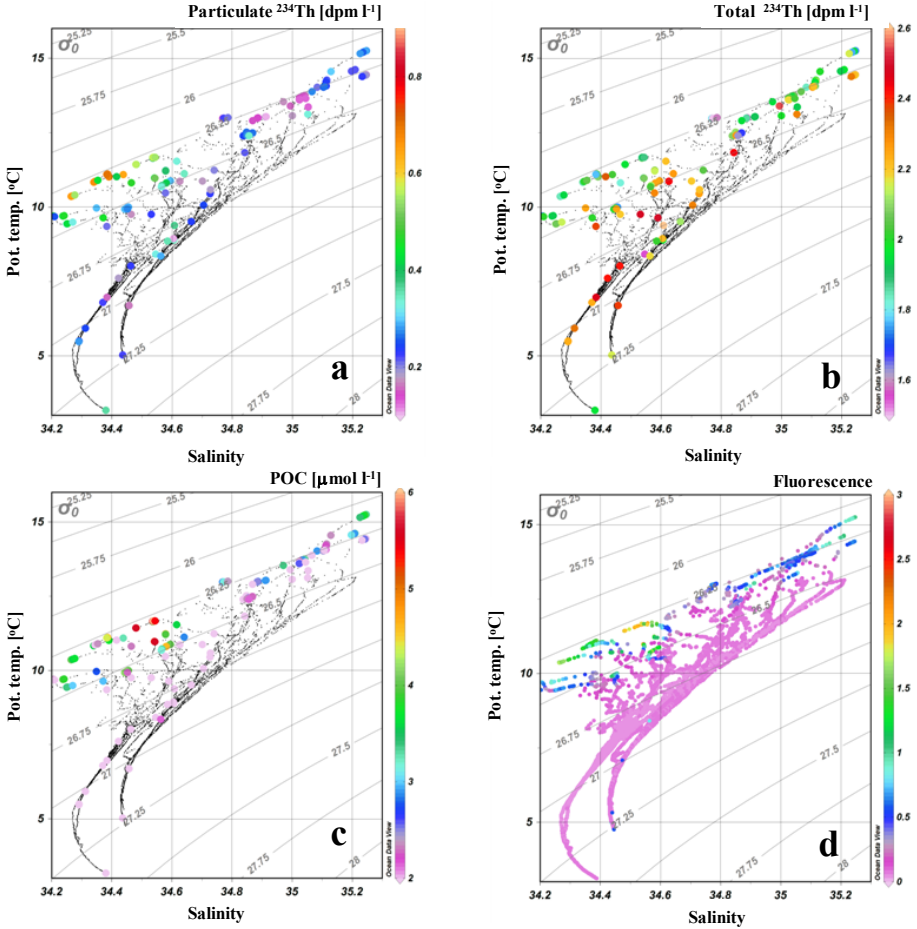

Fig. 6. Regional distributions of: **(a)** particulate ^{234}Th, **(b)** total ^{234}Th, **(c)** particulate organic carbon, and **(d)** fluorescence plotted on a T-S diagram.

BGD
8, 9535–9576, 2011

Enhancement of export flux in the highly productive STF

K. Zhou et al.

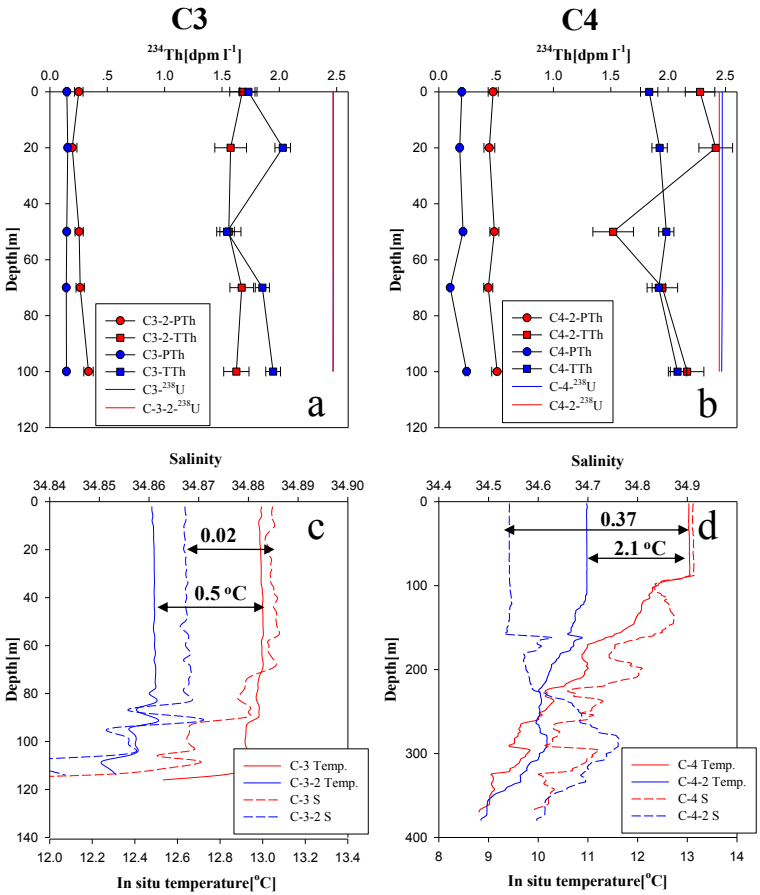

Fig. 7. **(a)** and **(b)** are vertical distributions of particulate and total ^{234}Th during the two visits to stations C3 and C4, with 16 days between C3 and C3-2 and 12 days between C4 and C4-2. **(c)** and **(d)** are vertical distributions of temperature and salinity at C3 and C4.

BGD
8, 9535–9576, 2011

Enhancement of export flux in the highly productive STF

K. Zhou et al.

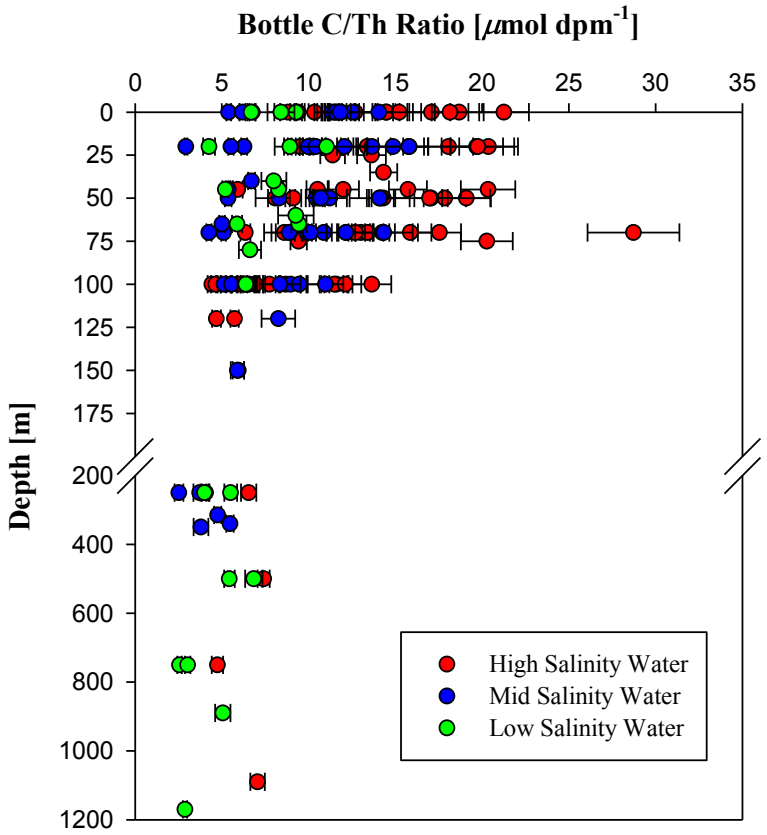

Fig. 8. Profiles of bottled POC/Th ratios for the three water types identified by their salinity differences (see Fig. 2).

BGD
8, 9535–9576, 2011

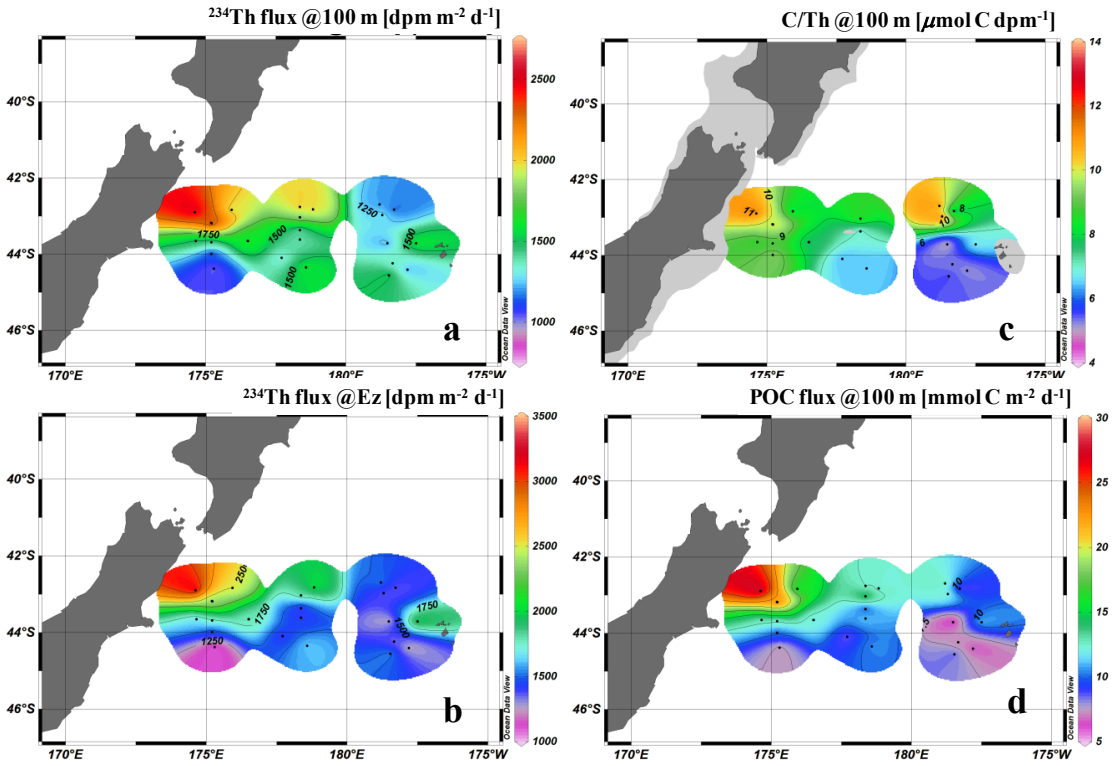

Fig. 9. Spatial distributions of: **(a)** ^{234}Th fluxes at 100 m depth, **(b)** ^{234}Th fluxes at Ez depth, **(c)** POC/Th ratio at 100 m, and **(d)** POC fluxes at 100 m.

BGD
8, 9535–9576, 2011